IMPERIAL COLLEGE LONDON

Department of Earth Science and Engineering

Centre for Petroleum Studies

J-Block Triassic Well Performance & Reservoir Heterogeneity

By

Akash Patel

In Conjunction with ConocoPhillips UK

A report submitted in partial fulfilment of the requirements for the MSc and/or the DIC.

September 2011

DECLARATION OF OWN WORK

I declare that this thesis

"J-Block Triassic Well Performance & Reservoir Heterogeneity"

is entirely my own work and that where any material could be construed as the work of others, it is fully cited and referenced, and/or with appropriate acknowledgement given.

Signature:.....…….

Name of student (Please print): **Akash Patel**

Name of supervisor: **William Beveridge, Hugo Lawrence (ConocoPhillips UK)**
Dr Jonathon Carter (Imperial College London)

Acknowledgements

First and foremost I would like to express my sincere gratitude towards my industry supervisors, William Beveridge and Hugo Lawrence for their invaluable help and guidance throughout the project and the J-Block Subsurface team for making this an enjoyable experience.

I would also like to thank my university supervisor, Dr Jonathon Carter for his kind supervision during the project.

Finally I would like to thank Andy Scott for making this opportunity possible with ConocoPhillips.

Contents

List of Figures

List of Tables

Imperial College London

J-Block Triassic Well Performance & Reservoir Heterogeneity

Akash Patel

Imperial College supervisor: Dr Jonathon Carter

Industry supervisors: William Beveridge, Hugo Lawrence (ConocoPhillips UK)

Abstract

Characterising Triassic fluvial high pressure high temperature reservoirs is a major challenge in the North Sea. The J-Block area, located north east of Aberdeen experiences a significant 'disconnect' between dynamic and static information. Dynamic data from drill stem test (DST) and back pressure techniques have proved that the effective kh is a magnitude lower than the estimates from core and log data. This significant difference in kh from core to DST scale suggests that heterogeneity may not be properly captured in the reservoir models.

This paper attempts to model heterogeneity at a very fine scale, similar to the dimensions of core plugs where 1ft*1ft*1ft grid blocks have been used. A number of facies realisations have been created by using property variograms to change facies dimensions and proportion. A pressure difference was created between two sides of the grid by using aquifers so that the effective permeability of the model could be back calculated from Darcy's equation. The effect of facies correlation lengths on the effective permeability of grid was compared to the core data. The main conclusion was that fine scale heterogeneity does not sufficiently explain discrepancy between effective field scale permeability and core plug poroperm data using these modeling techniques.

Two DST were carried out on the 30/2C-4 Jade appraisal well, one in the upper (DST2) and the other in the lower Joanne (DST1) which confirmed the hydrocarbon types and flow rates. A compositional model was built to simulate larger scale sand body distribution and to simulate history of the DST data after incorporating geological (stochastic realisations), petrophysical and reservoir engineering data. Sensitivities were also carried out to understand the influence of Kv, Kh, Skin and local grid refinement (LGR) on the pressure build up (PBU) and the corresponding well test derivatives.

A match to the actual data could not be obtained without the use of severe kh and kv multipliers, even with changes in facies correlation lengths, skin and LGR. The simulation responses of the two DST showed different behaviour, the lower Joanne simulation response requiring greater Kxy permeability multiplier than the upper Joanne. Several reasons for not being able to simulate the DST responses could be due to sub-seismic faulting and poor connectivity of the sand not captured by the modelling techniques used.

Introduction

J-Block is located approximately 130 km east of Aberdeen in the UK Central North Sea (Figure 1). J-Block fields produce volatile oil and gas condensates from HPHT reservoirs. The main producing reservoirs are the Cretaceous Chalk (in Joanne field) and the Triassic Judy and Joanne members of the Skagerrak formation in Jade and Judy fields. Jasmine field is currently under development and will produce from Joanne member sandstones. Jade was discovered in 1996 from the 30/2C-3 well which passes through the upper and lower Joanne sandstone. These are the two main productive reservoir units which are of the Triassic age and up to 1000 ft thick. The Judy sandstone member (thicker hydrocarbon column) is deepest and is separated from the Joanne by the Julius mudstone which is approximately 300 ft thick. Drill stem tests (DST) have been conducted on the 30/2C-4 well which confirmed flow rates in the upper and lower Joanne sandstones and also defined two different PVT regions in Jade. DST1 produced from the lower Joanne and DST2 produced from the upper Joanne. The main reservoir properties are listed in Table 1.

HC type	Gas condensate
Initial pressure	12,050-12,550 psia
Temperature	330-380°F
column height	3,300 ft tvd
Gas SG	0.9-1.35
GOR (scf/bbl)	5,200 – 15,200
CGR (bbl/mmscf)	65-192

Table 1: Main Jade Reservoir Properties

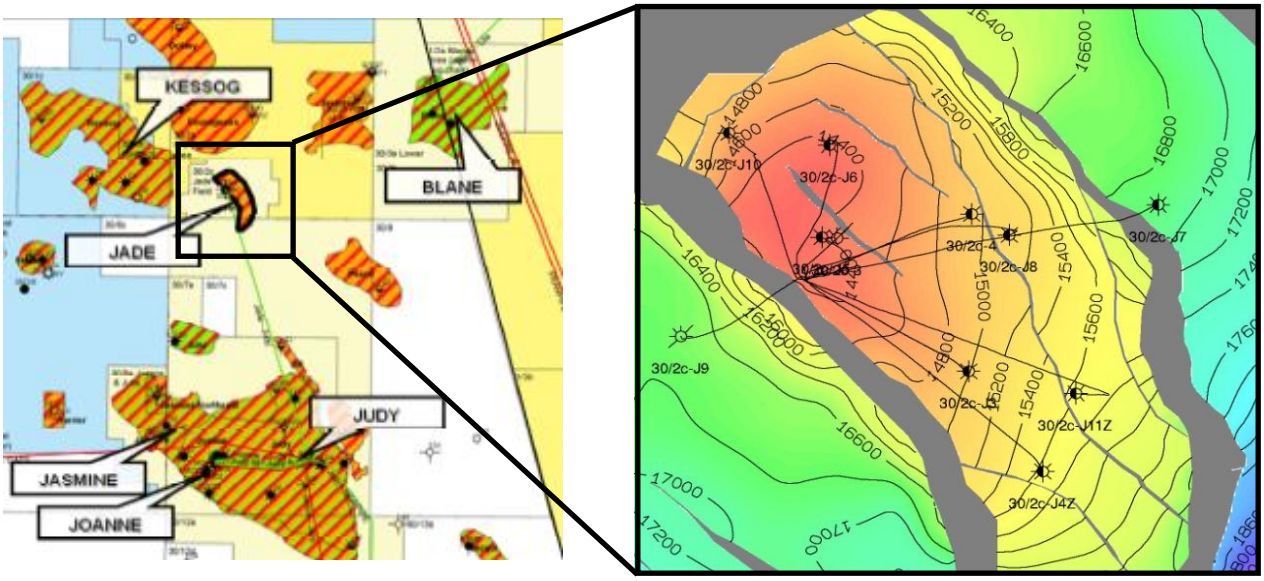

Figure 1: J-Block Area Overview (left)and neighbouring reservoirs and Jade Reservoir, Top Triassic reservoir coloured in depth (right)

One of the major challenges of the J-Block Triassic reservoirs is characterisation of permeability with both geological and reservoir engineering data. These fields show a disconnect between the static permeability data (core plug data) and dynamic permeability information (back pressure techniques and DST). Dynamic information has been observed to show a significantly lower effective kh than from the static data.

Well performance analysis using back pressure techniques and DST analysis typically shows high mobility during early times which degrades continually as the radius of investigation increases (Figure 2). In the past, radial composite models and near wellbore faults have been used in analytical and numerical well test analysis (WTA) in order to match the DST data. The results indicate that heterogeneity begins to impact responses over tens of meters rather than hundreds of meters.

The ramp effect is a typical signature of well test derivative which is observed in geologically complex high net to gross commingled reservoirs and is shown as a half slope in a log-log plot (Hamdi 2011). Recent work carried out by Corbett et al 2011 discusses the combined effect of gas condensate fluid and geology on the transient pressure well test response for commingled braided fluvial reservoirs. It has concluded that geology can complicate the well test and make it difficult to interpret. The results show that decreasing sand body dimensions causes the derivative to shift upwards while maintaining the derivative ramp effect. This ramp effect is also increased when the vertical permeability is decreases (Hamdi 2011).

Other well test responses identified in high net to gross fluvial reservoirs include geoskin and geochoke. These responses depend on the reservoir geology and the degree of flow communication both laterally and vertically. Geoskin responses have the same well test signature as fractured reservoirs showing a negative skin during interpretation, this due to the high level of permeability that can be seen in a channel thalweg facies (Corbett 1996). This can occur when communication both laterally and vertically is good. Geochoke is characterised by a 'hump' on the derivative, and has been identified due to poor communication between channels (Corbett 2005).

It can be challenging to history match production data to full field models (3D geocellular models used for flow simulation) for the Triassic J-Block reservoirs due to these permeability discrepancies. To date, history match has been achieved by using multipliers (often radial) to significantly reduce the permeability. The reduction in permeability by these multipliers suggests that there is an order of magnitude in difference between the core phie-perm and full field grid block phie-perm relationship.

There are many references in the technical literature (Waite 2004) to inconsistency in the reservoir properties

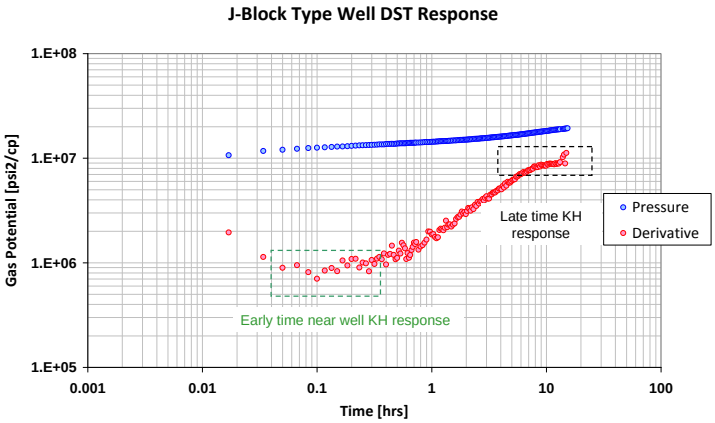

Figure 2: Typical fluvial Triassic pressure transient analysis response

from scaling; this is due to not properly taking into account the difference in scale between core plug measurement and model grid block. Core plugs measurements are in the centimetres whereas a single block maybe in the hundreds of feet in the horizontal direction and tens of ft in the vertical direction. Simulators are then used, which treat these coarse grid blocks as homogeneous volumes with uniform flow properties. However, in real cases the permeability can become more strongly anisotropic as volume support increases from core plug scales which are larger than the heterogeneity which affect fluid flow (Waite 2004). Instead of just deriving poro-perm relationships from core plug measurement scale and applying this to the full field models it has been suggested to use cloud transforms as part of the solution to the scale mismatch problem (Waite 2004).

A cloud transform is a porosity-permeability relationship that captures the spread/cloud of data points. The advantage of this approach over the conventional linear porosity-permeability technique is that it preserves the uncertainty in the bivariate relationship between porosity and permeability. Typically core plug data can show up to three orders of magnitude variation in permeability for a given porosity value, which is why cloud transforms may be appropriate as this variation in permeability is captured. These transforms can be easily developed by fitting permeability distributions to a range of porosity bins and then randomly assigning permeability to given porosity buckets according to probability distribution (Waite 2004).

Objectives

Ultimately, the objective was to develop a systematic methodology to characterise permeability for Central North Sea fluvial Triassic reservoirs from the core scale to the field modelling scale. The main objective of this was to investigate the causes of the discrepancy between the static description and dynamic information and recommend a modelling approach to match DST data.

Ultra fine scale geo-modelling was used to investigate how facies correlation lengths affect the effective permeability in a grid block that is equivalent to the size of single coarse cell. The main purpose of this was to determine if fine scale heterogeneity can explain the discrepancy between effective field scale permeability and core plug poroperm data.

The impact of using different methods to populate permeability in an intermediate size grid was also carried out, this looked at the differences between using linear poroperm relationships and cloud transforms. The simulation test were calibrated against DST data from the 30/2C-4 appraisal well to check for consistency with field pressure build up data.

Ultra Fine Scale Geo-Modelling

The main purpose of this section of the project was to recreate the fine scale level of heterogeneity (using 1ft grid cells) that exists in the Triassic sands for a range of facies realisations. This was achieved by using ultra fine gridding to model fine scale facies and property heterogeneity to capture the core plug poroperm relationship. A range of dimensions of fine scale heterogeneity were created in the geo-model to represent the scales at which they might exist. The objective is to determine what level of heterogeneity is important.

The workflow followed is described below,

- Develop very fine grid model and populate property heterogeneity using core plug data. Stochastic based modelling (SIS) was used to populate facies and sequential Gaussian simulation (SGS) for porosity.
- Create a pressure difference from two sides of the grid using two numerical aquifers with large pore volumes connected to the entire face and initiated at different pressures.
- Back-calculate effective permeability from Darcy's equation when steady state conditions are reached
- Upscale permeability using various averaging methods and compare

Grid and Aquifer Design

A simulation grid of size 160*160*20ft was constructed with individual cell sizes of 1*1*1ft in the x, y and z direction. The overall size of this grid represents a single coarse grid cell size. This is grid cell dimensions as used in recent coarse grid full filed model for an adjacent field. Two numerical aquifers with large pore volumes were attached to two opposite side of the grid in order to create a pressure difference in the model. The aquifers were initialised with different pressures.

Facies Modelling

Three facies types have been populated in the geo-model, these ranges from high to low reservoir quality and are sands, silts and shale's. Facies are discriminated in the model by applying volume-of-shale (Vsh) cut-off. This is based on the assumption that Vsh is an appropriate discriminator of grain-size and has been calibrated against core data. The facies were distributed within the reservoir by Sequential Indicator Simulation (SIS). A number of different facies realizations developed by changing the compositions of facies (see Table 2) and by also introducing facies variograms to create a range of possible reservoir descriptions (see Table 3). The shale content increases by 20% for each of the different cases so that barriers to flow both in the horizontal and

vertical direction can be modelled. The silt content is kept constant at 10% since this is less important for modelling barriers for flow. The major range shown in Table 3 represents the maximum correlation length in the horizontal direction whereas the minor range is the correlation length perpendicular to the major range. The vertical range is the vertical correlation length and controls the level of smearing. Variogram 1 represents the shortest correlation length and variogram 4 is the greatest correlation length, spanning outside the grid model.

Case	1	2	3	4
Sand %	70	50	30	10
Silt %	10	10	10	10
Shale %	20	40	60	80

Table 2: Four different cases with different facies content

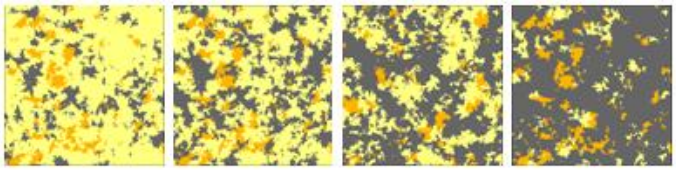

Figure 3: Increase in shale content (20% incrementally) from left to right

Variograms	Major (ft)	Minor (ft)	Vertical (ft)
1	16	16	2
2	40	40	2
3	160	160	2
4	200	200	2

Table 3: Different dimensional variograms applied to facies

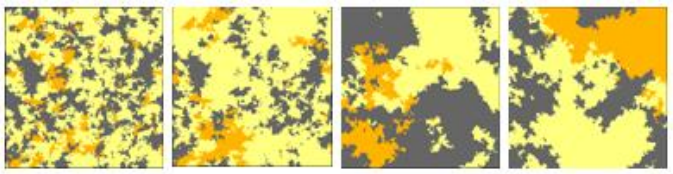

Figure 4: Increase in facies dimensions variogram from left to right

Porosity and Permeability Distribution

Porosity was distributed in the model by fitting a statistical distribution to each of the individual facies from the core plug data (see Appendix C for details). Poroperm cloud transforms based on the Jasmine/Jade core data have been used to populate permeability in the model, Klinkenberg corrected permeability was used and an overburden correction factor of 0.975 was applied for porosity. Porosity bins of approximately 1% phie were used to fit a trunclognormal distribution to the permeability scatter by using statistical analysis software, crystal ball (where the mean, standard deviation, minimum and maximum are defined) see Figure 5. Care is needed for this process, not only for selecting the size of the porosity bins but more importantly for eliminating any outlying core plug data. A single outlier with a magnitude of permeability difference can cause an unwanted and non representative cloud transform since the statistical distribution fitted to the data is skewed. A macro was generated and used to create the cloud transform (Figure 6), see Appendix E for example of poroperm cloud transform macro.

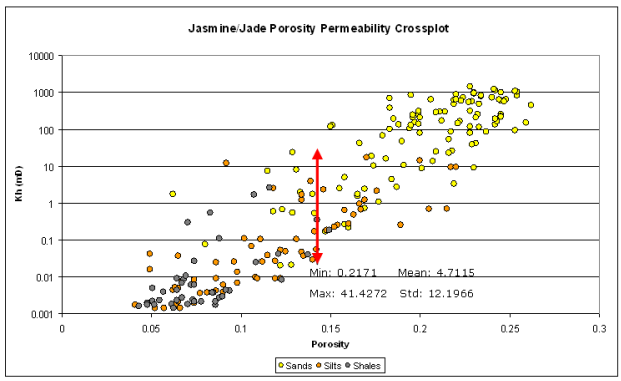

Figure 5: Core plug poroperm, TruncLogNormal distribution fit to permeability scatter

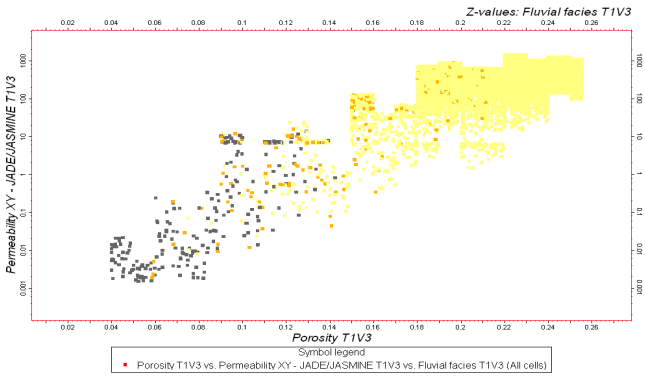

Figure 6: Fine scale model poroperm created from core plug data

A linear relationship between kv and kh was derived from using the core plug data and was based on the individual facie types, see Appendix C for details. It should be noted that with the limited data set used, the only a reliable correlation between kv-kh

was found to be for the sand facies. The correlation coefficient between kv and kxy for silts and shale was low. As a result of this uncertainty, sensitivity between kv and kxy were investigated.

Simulation and Upscaling

The effective permeability of the fine grid model was back-calculated from Darcy's equation (Equation 1) when steady state conditions were reached. This occurs when both aquifer flow rates are equal.

$$Q = \frac{-k.A.(P_b - P_a)}{u.L}$$

Equation 1: Darcy's Equation

where Q is the volumetric flow, k is the permeability, A is the cross sectional area, u is the viscosity, P is the pressure and L is the length. A pressure difference in the model created by the two aquifers is used to calculate the effective permeability in the ±I direction (Figure 7). Similarly aquifers were placed in the ±K direction to back calculate the effective permeability in the vertical direction.

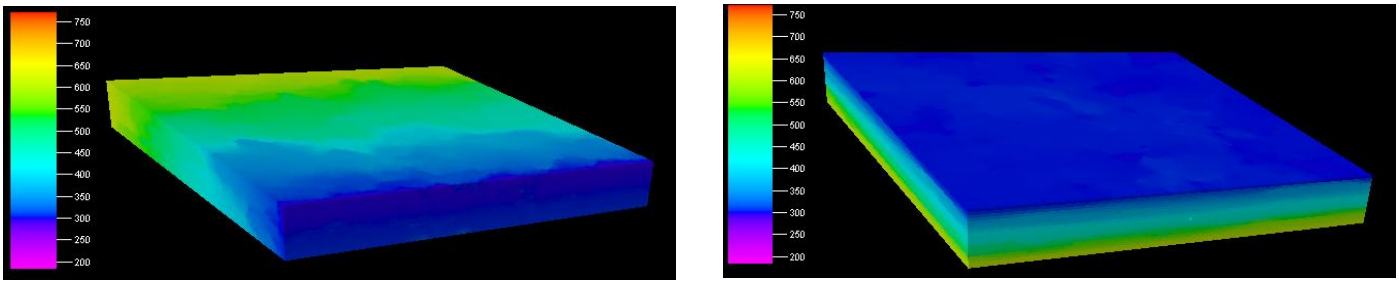

Figure 7: Ultra fine grid model showing pressure profile created by heterogeneity when steady state conditions are reached, this is created by aquifers in the ±I (left) and ±K direction (right), the colour bar shows the pressure in psia.

The model can then also be upscaled so that the arithmetic, geometric and harmonic permeability can be determined and compared to the back calculated effective 'dynamic' permeability. The choice of averaging is very significant as there are great variations between these methods. The arithmetic average is used for flow along layering and is weighted by the thickness, see Equation 2. The harmonic average is used for flow in series, such as vertical flow and is given by Equation 3. The geometric average lies between the arithmetic and harmonic, this averaging technique is normally used if permeability is randomly distributed (Equation 4).

$$K_{eff} = \frac{1}{H}\sum_{i=1}^{N} k_i H_i$$

Equation 2: Arithmetic average

$$K_{eff} = \left[\frac{1}{H}\sum_{i=1}^{N} \frac{H_i}{k_i}\right]^{-1}$$

Equation 3: Harmonic average

$$K_G = \prod_{i=1}^{N} k_i^{C_i}$$

Equation 4: Geometric average

Results

The results shown in Figure 8 are from using poroperm cloud transforms and individual facies to get relationships between kv and kxy. All the different realisations simulated are shown in the plot and it can be seen that the simulated effective permeability lies between the arithmetic and geometric averages, this result is expected. However, in comparison to the core data, the effective permeability generally lies at the high end (see Figure 9) and not the low end of the cloud. Some of the full field models used in the J-Block require permeability multipliers in order to reduce the permeability. This therefore suggests that there will is still be a order of magnitude in permeability difference from fine to coarse scale if the upscaled effective permeability transforms are used to populate permeability in the model. The results also show that the facies correlation lengths in high net sands do not make significant difference to the effective permeability.

The results also show that the appropriate permeability averaging method depends on the level of reservoir heterogeneity. It can be seen from Figure 8 that the effective permeability reflects more closely the arithmetic average when the sand to shale ratio is high. However as the shale content increases, this averaging method becomes more and more inaccurate and is better matched by the geometric average this result is also shown by Deutsch 1986.

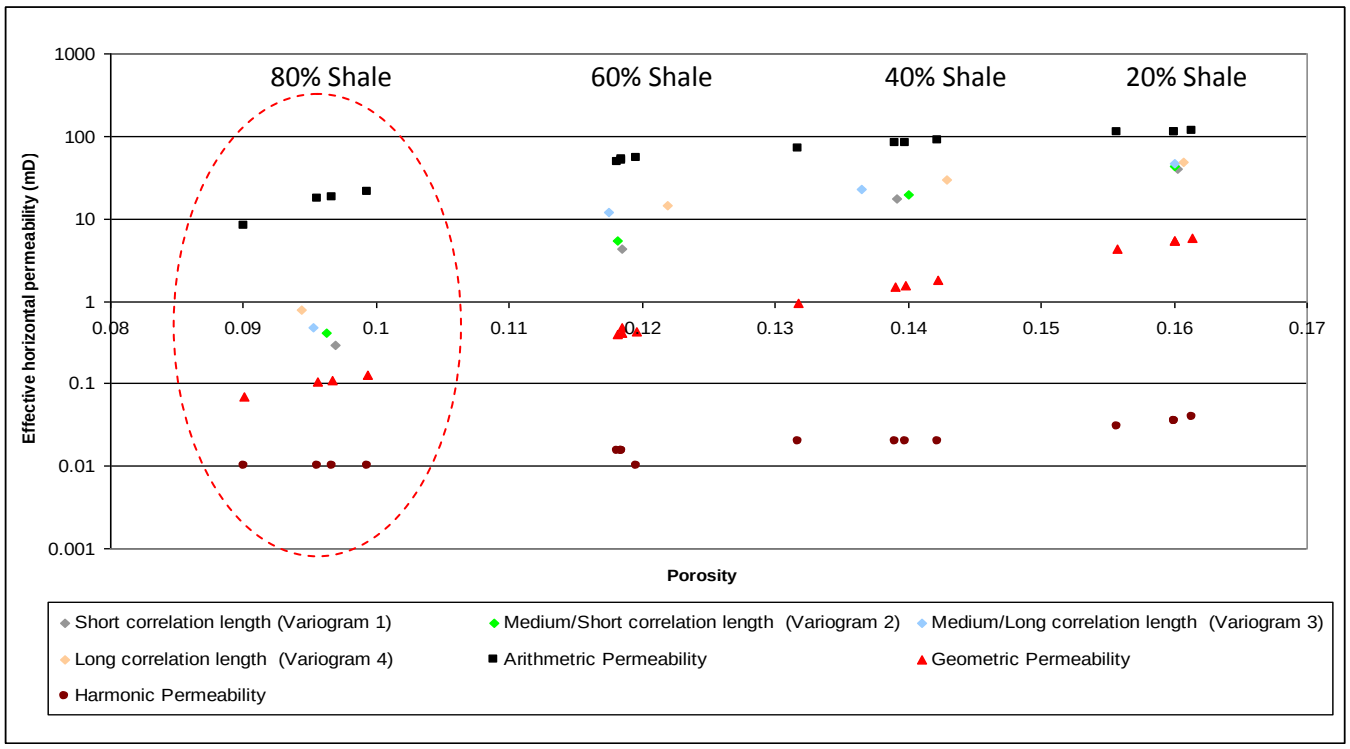

Figure 8: Simulated effective permeability and upscaled arithmetic, geometric and harmonic permeability. Decreasing porosity from right to left on the chart corresponds to increasing the shale volume; this is cases 1-4 from Table 2.

Due to the unreliable relationship between vertical and horizontal permeability from the core data, the vertical permeability was significantly lowered see the effect of preventing fluid from taking the 'easiest' route vertically (Figure 10). This modification of the kv-kxy relationships shows a significant difference from the initial results. The general trend observed is that as the shale proportion increases (moving from right to left on the porosity axis) there is greater variation between the original case and the modified case effective permeability. For high shale volume fractions of 60 and 80% (corresponding to approximately 9-10% and 12% porosity bins respectively in the plot) there is a magnitude in difference in effective permeability for the small correlation length facies.

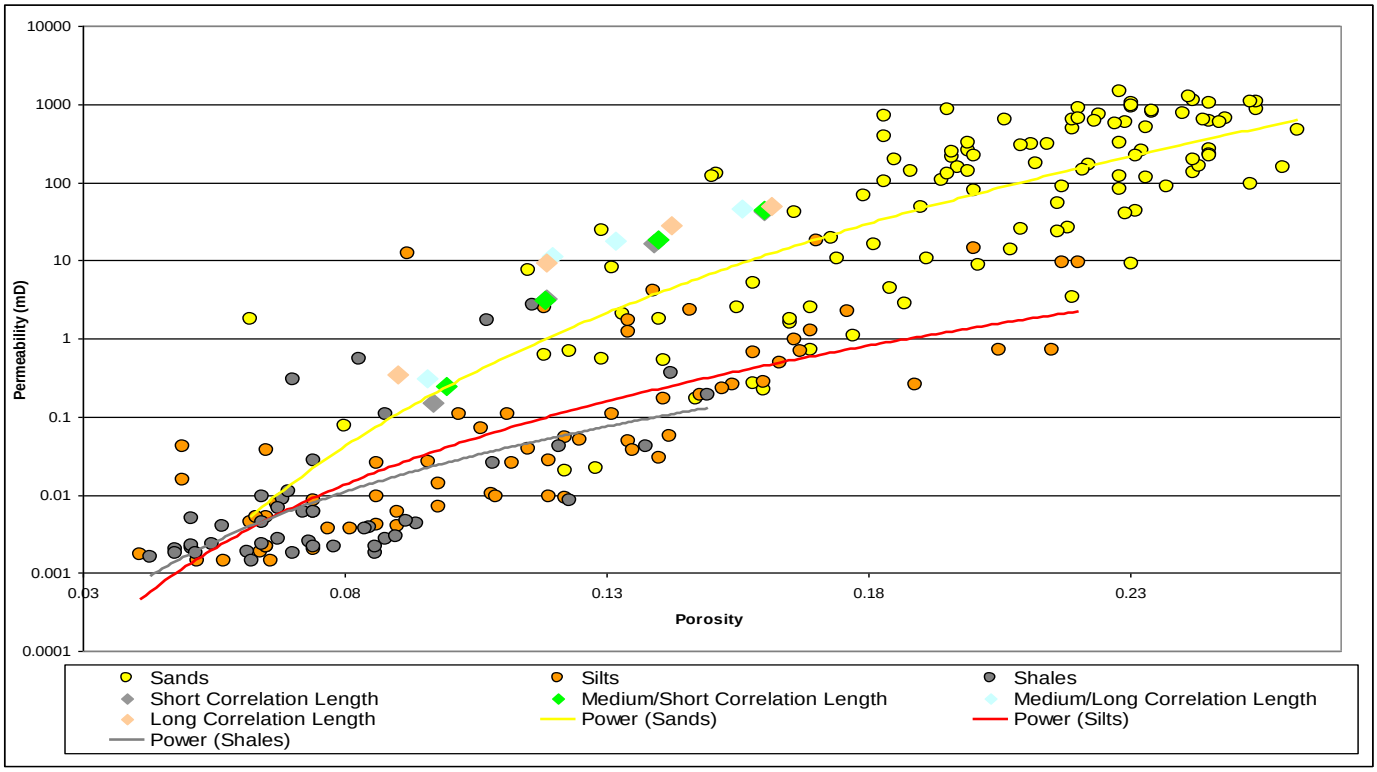

Figure 9: Back calculated effective permeability plotted against core data, points lie on the high side of the cloud

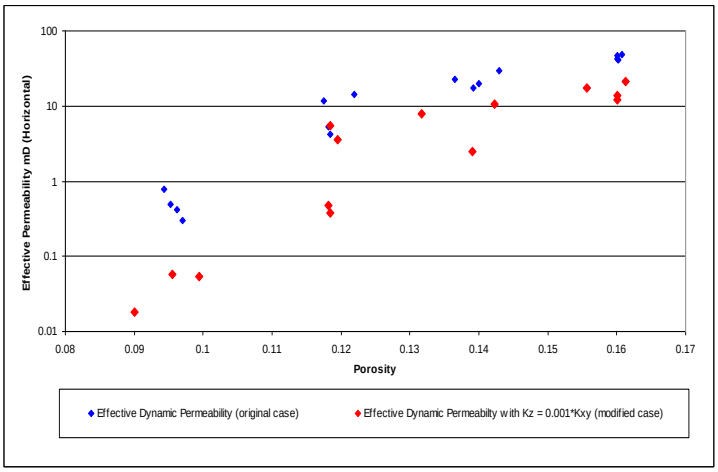

Figure 10: Comparison of effective dynamic horizontal permeability (Original case) with lowered Kv case

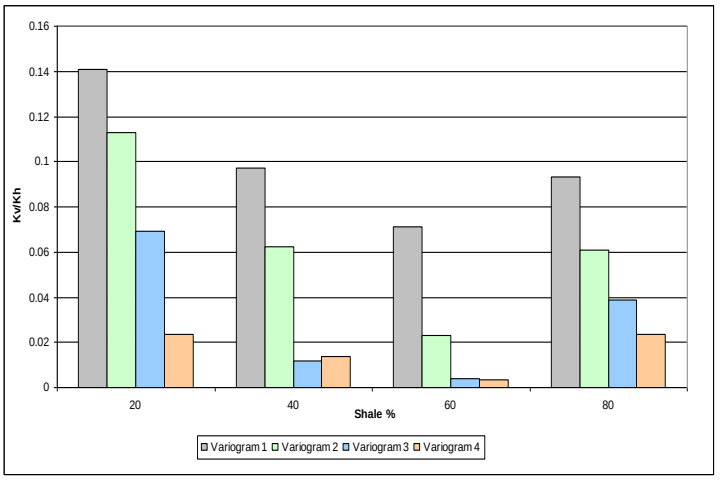

Figure 11: Shale proportion vs Kv/Kh ratio

Figure 11 shows the relationship between kv/kh and the shale proportions used to populate the model. The main result is that as the shale proportion increases the kv/kh ratio decreases until a certain point where then it increases, this relationship holds for all the facies variogram lengths. This is due to the increase in shale facies body as well as the rapid decrease in horizontal permeability.

Intermediate Model – DST Calibration

An intermediate sector model was built to test the short term well performance using DST 1 data from the 30/2C-4 appraisal well. The purpose of this section was to model larger scale sand body distribution at a coarser scale than in the previous model.

Workflow/Methodology

- Build detailed sector model which incorporates accurate descriptions of the fluid, rock and geological properties
- Use software package to simulate pressure build up (PBU) while history matching the flow response from the observed DST data
- Compare the simulated well test response with the actual DST data using well test package.
- If the simulated response does not match the observed response, use variograms to increase or decrease level of heterogeneity in model.

Simulation model description

A compositional numerical simulation model was built and was composed of 50*50*326 cells, each having dimensions of 20m*20m*4ft in the x, y and z direction respectively. A single partially penetrated vertical well (representing the 30/2C-4 well) located near the centre of a sector model was used in order to perform well test simulations while honoring the well data. This model forms part of a full field model which was populated with real reservoir properties from the Jade reservoir. Well test analysis for the 30/2C-4 well (DST1) gave an approximate value for the radius of investigation (Equation 5). This was found to be around 400ft. The total length of the sector model is 3280ft and therefore boundary effects were not anticipated in the sector model.

$$R_{inv} = \sqrt{\frac{k.t_p}{\phi.u.c_t}}$$

Equation 5: Radius of investigation

where R_{inv} is the radius of investigation (ft), k is the permeability (mD), t_p is the time (hours), ø is the porosity (fraction), u is the viscosity (cp) and C_t is the total compressibility (1/psi). The reservoir fluid properties for Jade were found to vary significantly from the upper to lower Joanne sandstones possibly due to the presence of a laterally extensive barrier. In order to model the DST responses, the sector model was split into two regions (Figure 12). The depths of these regions were taken from the 30/2C-4 well

log. The top of the upper and lower Joanne depths were taken at 14960 ft and 16270 ft MD respectively. Each region was assigned PVT properties corresponding to that of the actual test (see PVT model). To test the response of DST1 (lower Joanne), the well was perforated between depth intervals of 15645-15774 ft tvdss and between 15020-15065 ft tvdss for DST2 (see Figure 13).

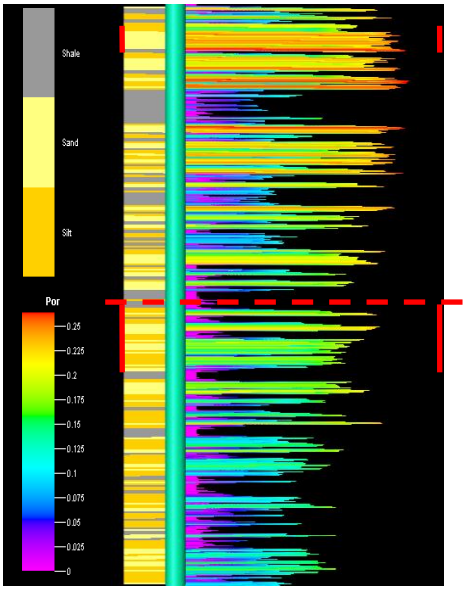

DST2 perforation (15020-15065 ft tvdss) penetrating a high porosity sand interval. Average porosity and permeability is 22.9% and 326.8mD respectively

Vertical Barrier separating the upper and lower Joanne

DST1 perforation (15645-15774 ft tvdss) penetrated mixed quality sands. Average porosity and permeability is 16.9% and 9.2mD respectively

Figure 13: Facie and porosity well logs for 30/2C-4 well

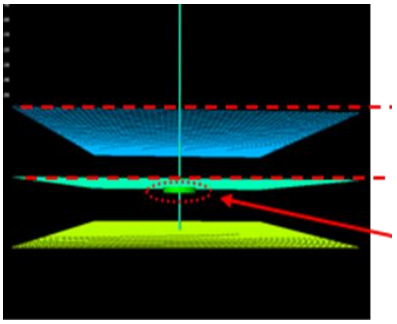

Upper Joanne

Lower Joanne

DST1 Perforation interval

Figure 12 : DST 1 Perforation zone penetrating the lower Joanne Sandstone

Facies Distribution

Three different facies have been assigned to the grid block models; these are channel sands, silts and shale as in the fine scale modelling. To honour the geology and petrophysical properties around the wellbore area, wireline data was used to create Vshale logs, in which facies logs were derived by applying Vshale cut-offs (Figure 13). The following Vshale cut-offs were applied, < 15%, >15 %< 40% and >40% for sand, silt and shales respectively.

Different realisations of facies distribution were created using the sequential indicator simulation (SIS) method. Five models were created in total with different facies variograms but all with the same proportion of facies, see table 4. Variogram 1 represents long facies correlations (also referred to as 100%since this is the longest correlation) and variogram 5 represents the shortest facies correlation lengths (10% of the longest correlation length). The azimuth and dip were kept at 0. The facies variograms used were kept the same for both the upper and lower Joanne and for all three facies types.

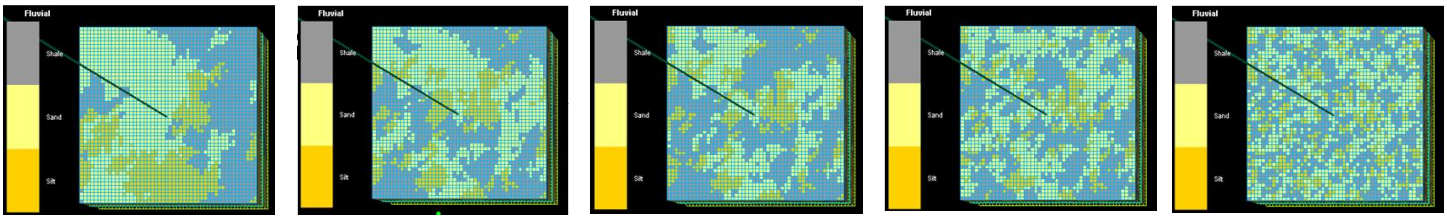

Figure 14: Multiple facie realisation created using variograms, long correlation lengths (left) to short correlation lengths (right)

Variogram	Major (ft)	Minor (ft)	Vertical (ft)
1 (100%)	1968	1312	32
2 (50%)	984	656	16
3 (30%)	590	393	9
4 (20%	393	262	6
5 (10%)	196	131	3

Table 4: Facies variograms used for generating different realisations for intermediate model

Porosity Distribution

Porosity was distributed in the sector model according to the facies type. Porosity statistics (mean, standard deviation, min and max) were determined for each of the facies type and populated using SGS.

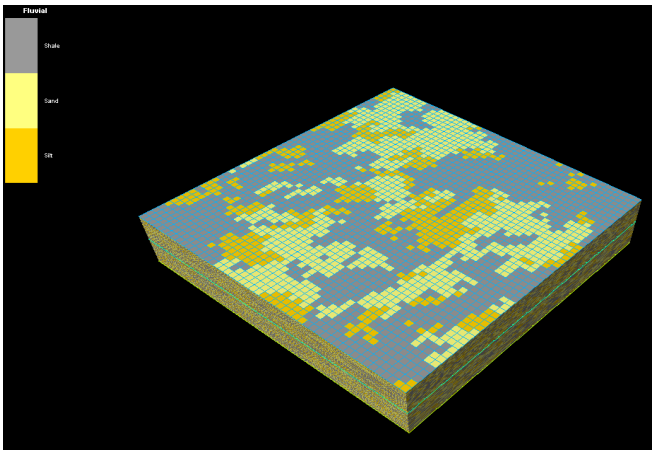

Figure 15: Facies populated in reservoir modelling using SIS method

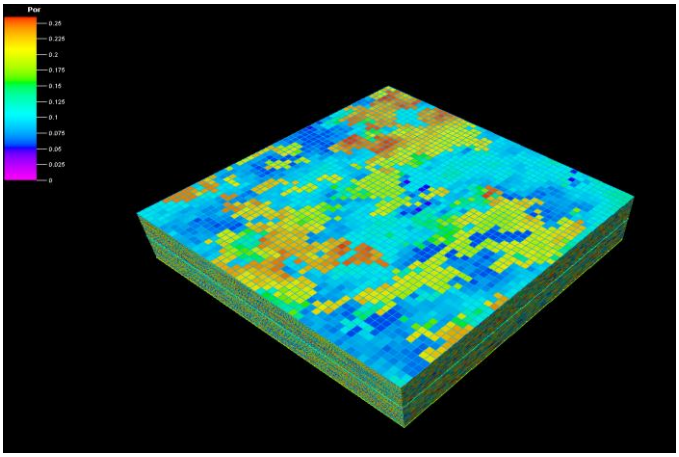

Figure 16: Porosity populated by facies in reservoir modelling using SGS method

Permeability Distribution

Core data from the Jade 30/2C-4 well was used to generate the cloud transform for the intermediate model so that permeability could be distributed. This data set reflects strongly that of the Jasmine/Jade used in the fine scale modeling. Linear poroperm relations were also used for each facies types as a comparison (see Appendix C for details, Figure C-7 and C-8).

PVT Model and DST

The DST from the 30/2C-4 appraisal well collected two fluid samples, one each from the upper and lower Joanne sands. PVT analysis showed that the fluid samples were unlikely to be in communication due to gravity segregation or thermal effects.

Peng-Robinson equation of state was used to describe the phase behaviour of the Jade 30/2C-4 DST 1 and DST 2 reservoir fluids. Individual EOS characterizations were conducted for each of the reservoir fluid and pseudoisation to reduce the equation of state into nine components. As these fluids can not be described with a single compositional gradient, the Joanne sands will have different PVT fluid regions in the simulation model.

The 30/2C-4 DST 1 sampled fluid between the depth interval 15645-15774 ft tvdss. The initial reservoir pressure and temperature was 12315 psia and 381°F respectively. The flowing period was conducted twice for this test; the first was for 9.5 hours and the second for 12 hours. The shut in times for the build up are 11 hours for first and second shut-in. 36/64 choke was used for the first flowing period which produced gas at an average rate of 25 MMCFD and oil at a rate of 4638 STBOPD. The second flow period used two different chokes, 48/64 and 40/64. The first choke averages gas at a rate of 30 MMCFD and oil at 5845 STBOPD. Finally the second choke averages gas at a rate of 24 MMCFD and oil at 4640 STBOPD.

DST 2 fluid sample was taken from 15020-15065 ft tvdss. Initial reservoir pressure and temperatures was 12165 psia and 370°F. The perforation interval for the test was between 15020 – 15065 ft tvdss. There were three flow periods and shut-in periods. The initial flow period was for 9 hours at two different chokes, 36/64 and 44/64 which produced gas and oil at a rate of 33 MMCFD 3000 STBOPD and 40 MMCFD 3600 STBOPD. The first shut-in period was for 12 hours. The second flow in period and shut-in was for 4 hours and 3 hours respectively due to problems with the separator. The last flow period was for 48 hours at three different chokes, 36/64, 40/64 and 48/64 produced gas and oil at a rate of 39MMCFD 2800 STBOPD, 44MMCFD 3050 STBOPD, and 57MMCFD 3750 STBOPD respectively.

Sensitivities studied

A series of sensitivities have been performed so that the use of cloud transforms can be compared to the linear poro-perm relationships. The sensitivities investigated are the effects of Kv, Kh, Skin and correlation length. Comparisons are made using both the pressure build up plot and the corresponding derivative.

DST1 Results

Case 1 (Lower Joanne Sandstone)

The first case involved two sets of runs, those using cloud transforms to populate poroperm and the other using linear poroperm relationships. The findings from the fine grid model (0.01 Kv/Kh ratio) and the Jade well/reservoir properties were used as the input for the runs. A total skin value of 3.7 was determined from transient pressure analysis for the 30/2C-4 well, this was applied in the simulation runs. No multipliers for kxy were applied. Results for the cloud transforms are shown below (Figure 17 and Figure 18) and are very similar to the results from the linear transform (details for linear transform sensitivities are given in Appendix C).

It can be clearly seen that no match to the actual DST data was found as very little drawdown is achieved for all five correlation lengths, however there is slightly more drawdown for the shorter correlation length facies. The derivative response is a flat, showing no sign of the 'ramp effect' that is seen in the DST 1 test derivative.

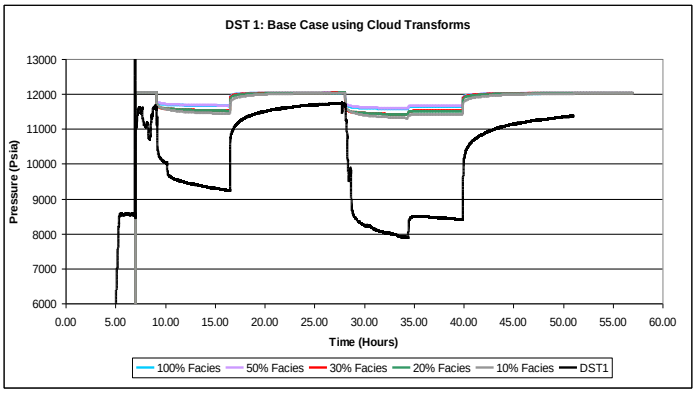

Figure 17: PBU plot of case 1 using cloud transforms

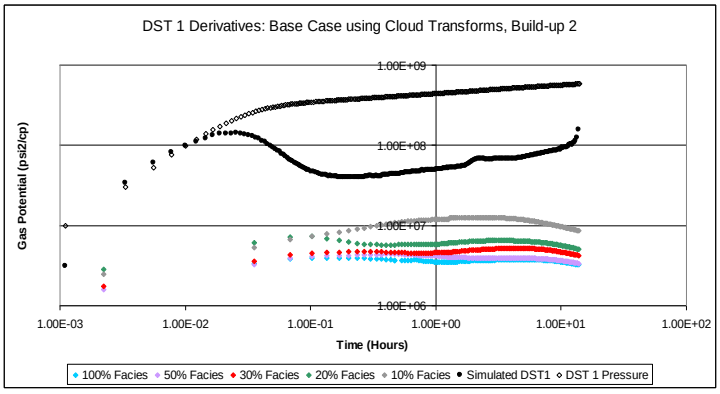

Figure 18: Derivative of case 1 using poroperm cloud transforms

Case 2- Addition of Kxy Multiplier

The same tests were run as in case 1 but manipulated with a 0.1 multiplier applied to Kxy. The addition of this multiplier was based on achieving a similar match to the actual pressure drawdown data. A significant difference can be seen in terms of the level of drawdown on the PBU plot and the appearance of the 'ramp effect' in the corresponding derivates for some of the smaller correlation length facies. Figure 19 and Figure 20 below are shown for the cloud poroperm transform runs. The 20% facies correlation length shown below in the derivative plot shows an unexpected and different shape to the others and can be explained due to the re-population of facies around well area. The main conclusion drawn between using cloud and linear transforms for this case is that there is more drawdown when linear transforms are used (details for linear transform sensitivities are given in Appendix C).

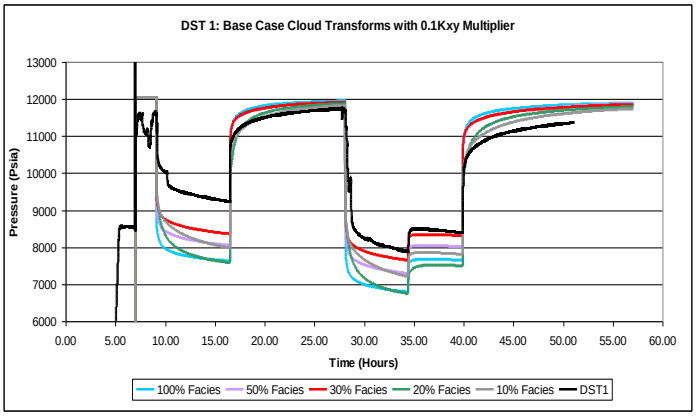

Figure 19: PBU of case 2 with 0.1 k_{xy} multiplier

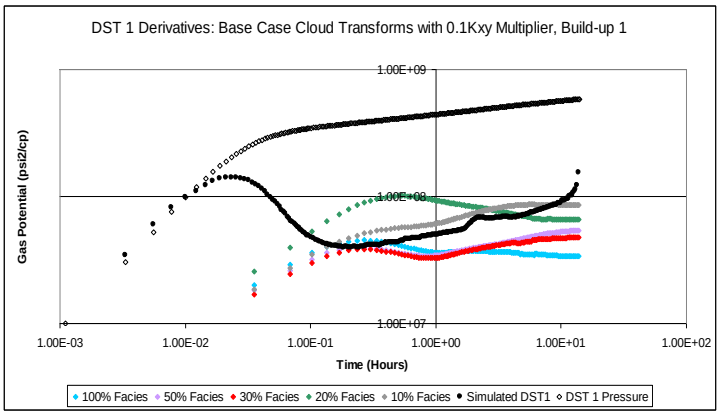

Figure 20: Derivative of case 2 using poroperm cloud transforms

For cases 3-6, medium facies correlation lengths (30%) were used to perform sensitivity analysis on.

Case 3 - Vertical permeability (Kv) Sensitivity Analysis on Case 2

A step-wise decrease in Kv was taken to find out the effect on the well test derivative with 30% of the original correlation length. The same trend was observed for both cases, using linear and cloud transforms. A decrease in Kv lowers the drawdown in the PBU plot and increases the derivate ramp effect (Figure 21 and Figure 22) confirming conclusions from Corbett's et al work. Decrease in Kv causes the ramp effect to disappear. Details for linear transform sensitivities are given in Appendix C

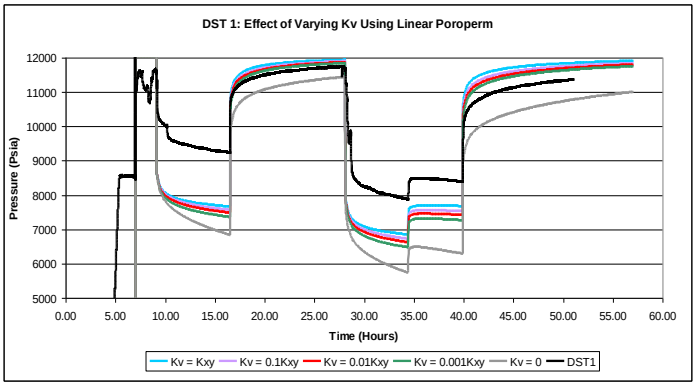

Figure 21: PBU of case 3 showing vertical permeability sensitivity

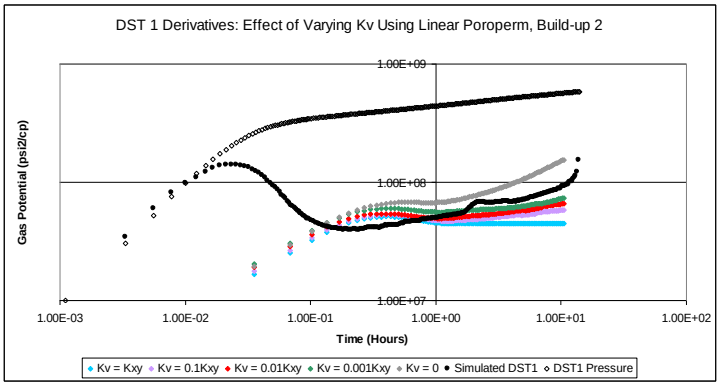

Figure 22: Derivatives of case 3 showing vertical permeability sensitivity

Case 4 - Horizontal permeability (K_H) Sensitivity Analysis on Case 2

Magnitude in changes of KH causes significant changes to the pressure build up, drawdown and to the corresponding derivative shape (Figure 23 and Figure 24). Decreasing Kxy lowers the pressure drawdown (in extreme cases where 0.001 multiplier is used, the flow in bottom hole pressure is zero) and seems to increase the ramp effect at both middle times and late times.

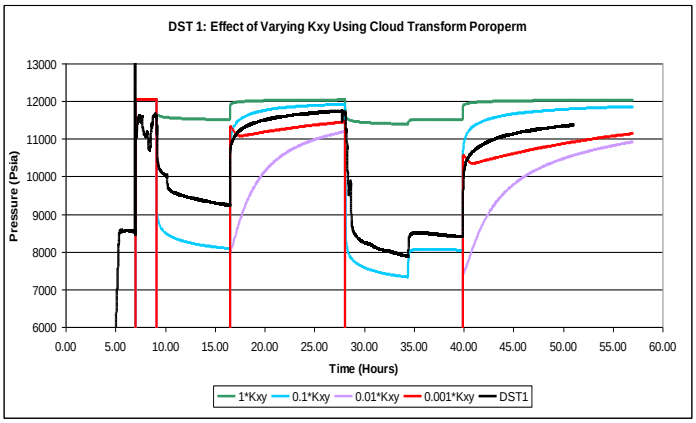

Figure 23: PBU of case 4 showing horizontal permeability sensitivity

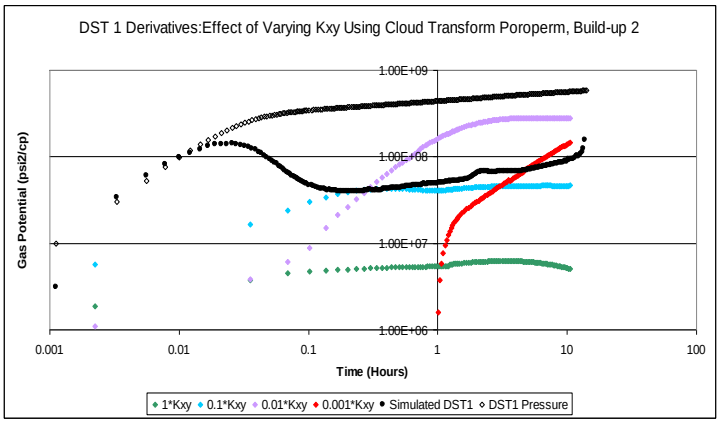

Figure 24: Derivatives of case 4 showing horizontal permeability sensitivity

Case 5 - Skin Sensitivity based on Case 2

Five different total skin conditions were run ranging from -2 (completed) to +10 (damaged). Increasing skin increases the drawdown and has no effect on the derivative as expected for both the cloud and linear transform. The plots below are shown for the poroperm cloud transform runs (details for linear transform sensitivities are given in Appendix C).

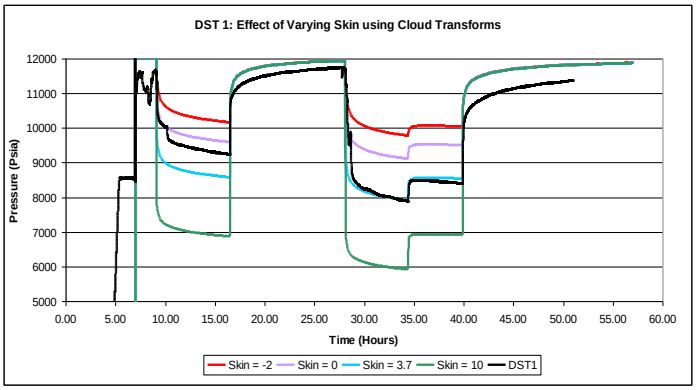

Figure 25: PBU of case 5 showing skin sensitivity

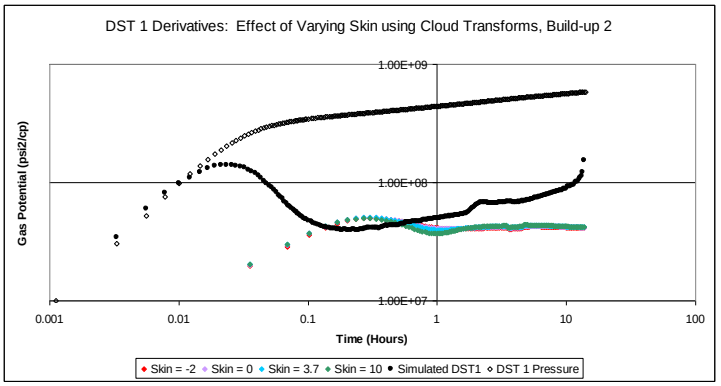

Figure 26: Derivatives of case 5 showing skin sensitivity

Case 6 - Local Grid Refinement Sensitivity on Case 2

Local grid refinement was applied around the wellbore to reduce numerical artefacts that may appear in well test derivative responses. Several sensitivities have been run to test the effect of LGR on the history matched PBU and well test derivative; see Figure 27 and Figure 28. Increasing LGR decreases the drawdown on the PBU plot when cloud transforms are used. When LGR is used with cloud transforms, it can be seen as increasing the level of heterogeneity in the model since the TruncLogNormal function assigns a statistically fit distribution to a porosity value (ie there is no single permeability value for a porosity). An increase in LGR causes an increase in the derivative but does not add to the ramp effect. No significant difference is made when this exercise is repeated using linear poroperm relationships since the cells in the LGR have the same porosity value as the parent cell and same permeability value as a result. This demonstrates that numerical dispersion is not an issue

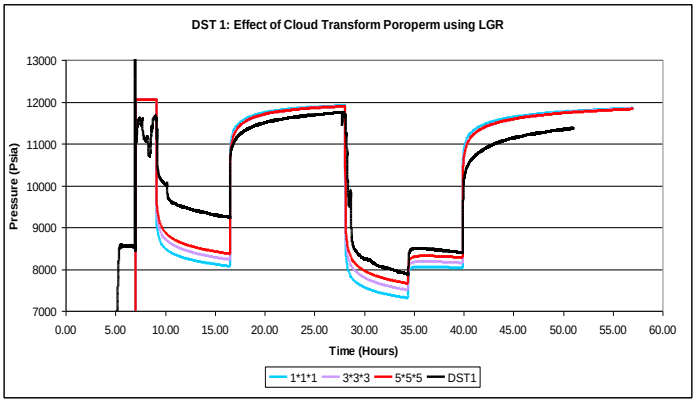

Figure 27: PBU of case 6 showing LGR sensitivity

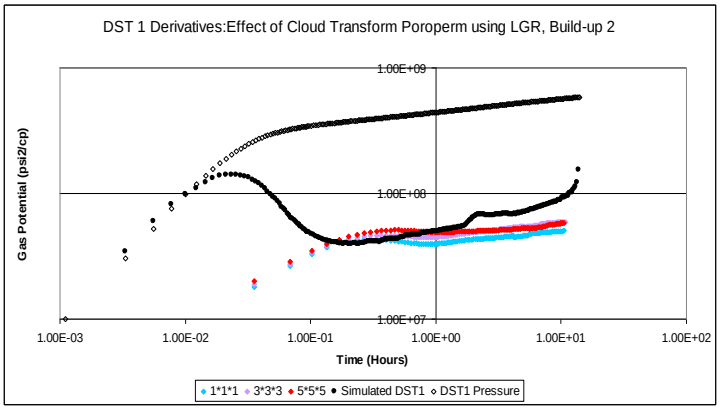

Figure 28: Derivatives of case 6 showing LGR sensitivity

DST2 Results (Upper Joanne Sandstone)

A similar approach to the first DST was taken to evaluate the effects of skin, horizontal and vertical permeability for the upper Joanne sandstone. Only cloud transforms have been used to populate permeability in the model since the differences between using linear and cloud transform have already been explored.

Case 1

Well test analysis for DST2 revealed that poor completions procedures were used and thus reported a total skin value of 10. This skin, along with the 0.01 Kv/Kh ratio (from the fine grid model) and cloud poroperm transform was used as a starting point to simulate the DST response. Again the results were not too dissimilar to that of the DST1; this is that not enough drawdown is achieved in the simulation (Figure 29and Figure 30).

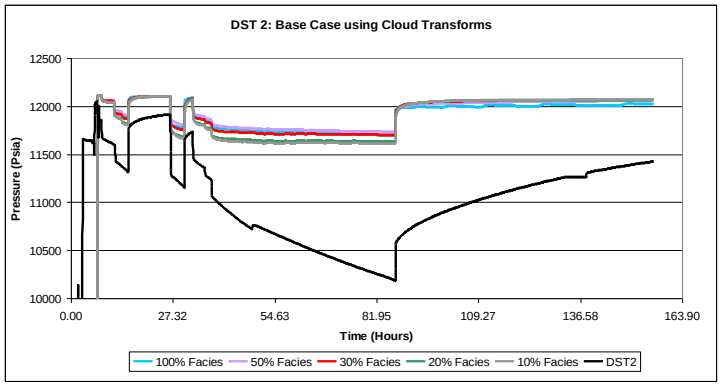

Figure 29: PBU of case 1 DST2 showing sensitivity of 5 different correlation lengths without use of multipliers

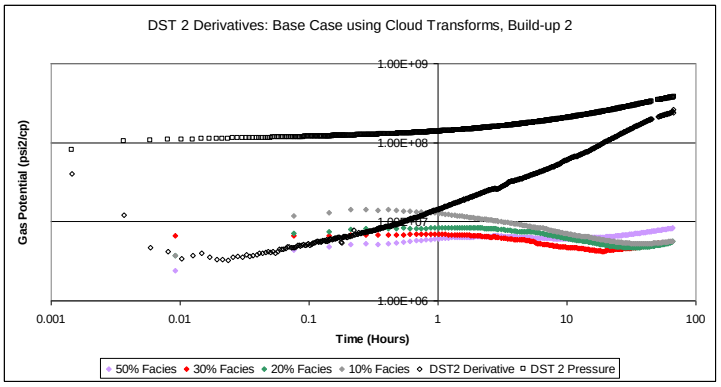

Figure 30: Derivatives of case 1 DST2 showing sensitivity of 5 different correlation lengths without use of multipliers

Case 2

Again, a multiplier was applied to the horizontal permeability to try achieving the appropriate level of drawdown that is received in the actual DST2 data (Figure 31). A 0.3 multiplier to all the facies correlation lengths seems to give the closest response. The corresponding derivative for the final build is shown below (Figure 32) and is far from simulating the actual DST, it can also be seen in the PBU plot that last build up shape of all the correlation lengths is much different from the actual test.

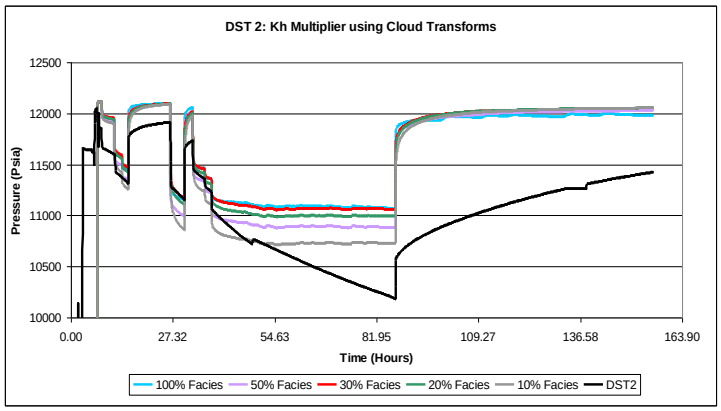

Figure 31: PBU of case 2 DST2 showing sensitivity of 5 different correlation lengths with use of multipliers

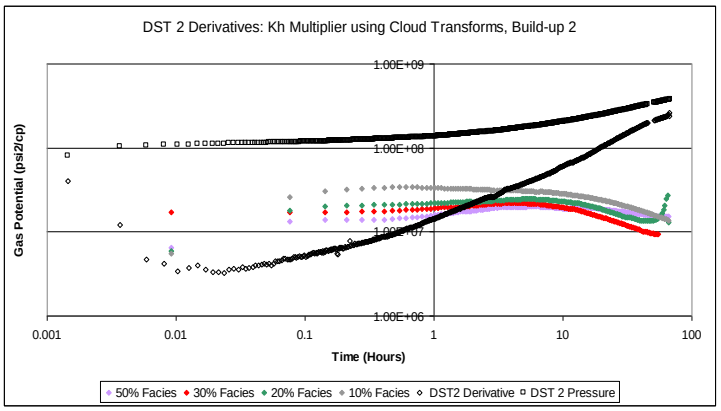

Figure 32: Derivatives of case 2 DST2 showing sensitivity of 5 different correlation lengths with use of multipliers

Case 3

Sensitivity on Kv was again looked at with the 0.3 kxy multiplier and 30% correlation length facies. As before, the only real scenario that made a difference to the PBU was when the vertical permeability was set to zero. This test for the first time simulated a similar shape response to the third pressure drawdown and the final build up (Figure 33). When this is compared to the derivative (Figure 34), the 'ramp' effect is simulated, but however is far from close the to the actual DST response.

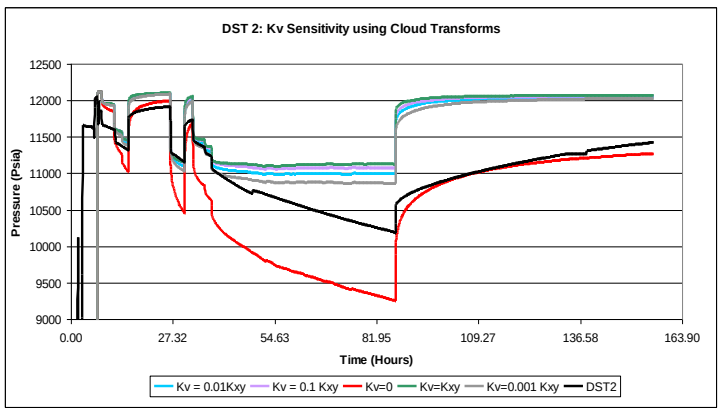

Figure 33: PBU of case 2 DST2 showing sensitivity of vertical permeability

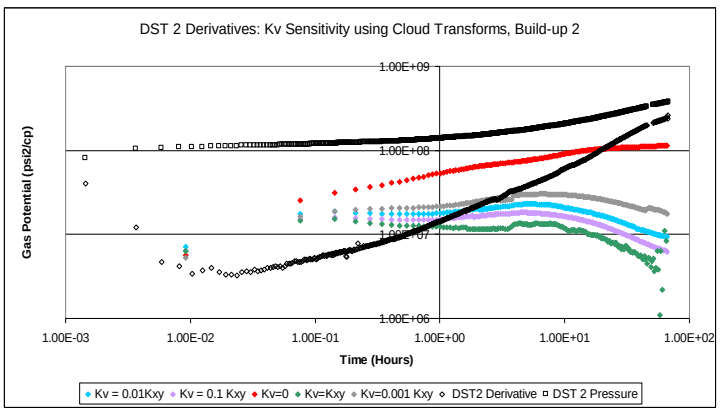

Figure 34: Derivatives of case 2 DST2 showing sensitivity of vertical permeability

Conclusions

Ultra fine scale heterogeneity modelling was investigated using 1ft*1ft*1ft grid cells. Core plug data from Jasmine/Judy filed was used to populate permeability in the simulation model. Two cases were looked at, where core plug kv-kh relationship was used and a modified case with a much lower kv/kh. The effective permeability of the model was compared to the core plug poroperm data.

The conclusions of the study are:

- Fine scale heterogeneity does not explain discrepancy between effective field scale permeability and core plug poroperm data when poroperm kh and kv relationship is used (from Jasmine/Judy data set)

Possible explanations include,

- Modelling approach using elliptical sand bodies does not capture the character of fine scale heterogeneity
- Core plug poroperm are not representative or misleading
- Current grid cell size may not be small enough to capture heterogeneity

When the vertical permeability is significantly lowered (justified on the basis of unreliable kv-kh relationship since this shows a weak correlation between the data sets) a magnitude difference in permeability is observed for the high shale (60-80%) and short facies correlation length models.

A coarser grid block model was built using grid cell sizes of 20m*20m*4ft to investigate the impact of larger sand body distribution on simulating the DST responses using both poroperm cloud transforms and linear poroperm relationships. Sensitivity was carried on kh, kv, skin and local grid refinement to see the effect on the PBU and the well test derivative.

The main conclusions of the second part of the study are:

- Facies variograms alone cannot help achieve a match between the Jade sector model and either of the actual DST data from the 30/2C-4 well, this is because enough drawdown is not simulated in the model
- Kh multipliers are needed to get a similar level of drawdown for both the DST, a smaller multiplier is required for DST1 (approximately 0.1, whereas DST2 is 0.3)
- Better simulation response is observed with very low kv in the coarse grid model (simulating the ramp effect), this is consistent with the fine grid model results where a magnitude difference in permeability is observed with the kv significantly lowered.
- The log data from DST2 (upper Joanne sandstone member) indicates that the perforated interval is of very good reservoir quality, possibly intersecting a sand channel. However the DST2 simulation responses indicate that the reservoir undergoes pressure depletion very quickly whereas the actual test data does not, indicating the possibility of extensive lateral barriers/shales.

The overall conclusions of the study are the coarse grid model requires very low kv to simulate the ramp effect, this kv is even lower than that from the fine grid model and the kv/kh pairs. This analysis suggests that vertical barriers are not captured in either the ultra fine or intermediate grid models.

Recommendations

As described earlier, the statistical modelling of the cloud transform plays an important part in determining the effective permeability. Introducing a density function into simulators for the generation of poroperm cloud transforms would be beneficial to prevent unwanted skewing. This unwanted skewing is shown at the high end of the sand facies of the cloud transform that was used in this study.

In this project stochastic based facies modelling was used to try and understand how certain variables can affect the pressure build up and the corresponding well test derivative. Other geological variables could be incorporated into the simulation model to try and get a better simulation response with both of the DST data sets by investigating the effects of near wellbore and sub seismic faulting with a range of transmissibility factors. As further work, multipoint statistics or object based modelling could be approached to try and better understand the reservoir geology since a sand channel may be present from DST2 according to the

log data. These channel sands could be populated in the model with sensitivities applied to the height/width ratios as well as changes in channel sinuosity.

Only the short term well performance from the DST has been simulated using the coarse grid model. It is recommended that this is simulated against long term production history so that the affects of multiphase flow around the wellbore region (when pressures drop below the dew point) can be evaluated since the J-Block reservoirs are gas condensates.

Nomenclature

A = Area, ft
C_t = Total compressibility, 1/psi
K_{eff} = Effective permeability, mD
K_G = Geometric permeability, mD
Kv = Vertical permeability, mD
K_h = Horizontal permeability, mD
kh = Permeability height mD.ft
L = Length, ft
R_{inv} = Radius of investigation, ft
P = Pressure, psi
Q = Volumetric flow rate, ft
S = Skin
t_p = Time, hours
u = Viscosity, cp
ø = Porosity, fraction

Abbreviation

LGR = Local Grid Refinement
PBU = Pressure build up
PVT = Pressure, Volume and Temperature
DST = Drill Stem Test
EOS = Equation of State
GOR = Gas to oil ratio
HPHT = High Pressure High Temperature
SIS = Sequential Indicator Simulation
SGS = Sequential Gaussian Simulation
WTA = Well Test Analysis
MMCFD = Million cubic foot per day
STBOPD = Stock tank barrel oil per day

References

Corbett, Patrick W.M., Heriot-Watt University; Mesmari, Abdallah, Agip Oil Co.; Stewart, George, Edinburgh Petroleum Services Ltd. 'A method for using the naturally-occurring negative geoskin in the description of fluvial reservoirs', SPE 36882 (1996)

Corbett, Patrick W.M, Hamidreza Hamdi, Hermant Gurev, 'Layered Reservoirs with Internal Crossflow: A Well-Connected Family of Well-Test Pressure Transient Responses', Institute of Petroleum Engineering, Heriott-Watt, Edinburgh, Riccarton. Presented at the AFES seminar, 'Well Testing for Reservoir Description'

Corbett, Patrick W.M, SPE, Y. Ellabad, J.I.K. Egert, and S. Zheng, SPE, Heriot-Watt U. , 'The geochoke well test response in a catalogue of systematic geotype curves', SPE 93992-MS (2005)

Deutsch, C., Desbarats, A.J, Journel, A.G., Stanford U. Power Averaging for Block Effective Permeability, SPE California Regional Meeting, 1986, SPE 15128-MS

*Eamon Marron, Iain Mearns, ConocoPhillips UK, Jasmine Permeability Modelling, April 2006 (ConocoPhillips internal report)

H. Hamdi, M. Jamiolahmady and P.W.M. Corbett, Heriot-Watt U. 'Modelling the Interfering Effects of Gas Condensate and Geological Heterogeneities on Transient Pressure Response' , SPE 143613-MS (2011)

M. Waite, S Johansen, D. Betancourt, U Acharya, 'Modeling of scale-dependent permeability using single-well micro-models: Application to Hamaca Field, Venezuela' , SPE 86976 (2004)

*R. L. Bone, Jade Field Equation-of-State development 2004, ConocoPhillips

*Shi-YI Zheng, Patrick W. M.Corbett, Alf Ryseth and George Stewart, Uncertainty in well test and core permeability analysis: a case study in fluvial channel reservoirs, northern North Sea Norway, AAPG Bulletin, v.84, No.12 (December 2000), pp. 1929-1954

*T. Ariadji, Bandung Inst. of Technology; H. Suryanto, ConocoPhillips; and S. Mariani, Bandung Inst. of Technology, 'Reservoir Characterization Through A Single Well Numerical Study Using DST Matching for A Gas Condensate Reservoir', SPE 93218

*Toro-Rivera, M.L.E., Corbett, P.W.M., Heriot-Watt U.; Stewart, George, Edinburgh Petroleum Services (EPS) Ltd, 'Well Test Interpretation in a Heterogeneous Braided Fluvial Reservoir', SPE 28828, 1994

Appendix A

Critical Milestones

SE Paper Number	Year	Title	Authors	Contribution
102093	2006	Three Statistical Pitfalls of PHI-K Transforms	P. Delfiner et al	Shows Swanson mean better represent poroperm data statistically
36882	1996	A method for using the naturally-occurring negative geoskin in the description of fluvial reservoirs	Corbett, Patrick W.M.	Using geoskin concept in fluvial reservoir description
86976	2004	Modeling of scale-dependent permeability using single-well micro-models: Application to Hamaca Field, Venezuela	M. Waite, S Johansen, D. Betancourt, U Acharya	High end point estimates for kv/kh ratio are produced when core based poroperm relationships are used at macro scale reservoir models.
93992-MS	2005	The geochoke well test response in a catalogue of systematic geotype curves	P.W.M. Corbett, SPE, Y. Ellabad, J.I.K. Egert, and S. Zheng, SPE, Heriot-Watt University	Using geochoke concept for fluvial reservoir characterisation
143613-MS	2011	Modeling the Interfering Effects of Gas Condensate and Geological Heterogeneities on Transient Pressure Response	H. Hamdi, M. Jamiolahmady and P.W.M. Corbett, Heriot-Watt U.	Increasing geology effect (heterogeneity) increases the 'ramp' response seen in fluvial reservoirs and shorter correlations lengths magnifies the ramp effect

Appendix B

Critical Literature Review

SPE 86976 (2004)

Modeling of scale-dependent permeability using single-well micro-models: Application to Hamaca Field, Venezuela

Authors: M. Waite, S Johansen, D. Betancourt, U Acharya

Contribution to the developing a workflow to upscale core plug phie-perm to macro scale by using cloud transform to preserve the uncertainty in the bivariate relationship between phie and k.

Objective of the paper: Solution to scale up core plug porosity permeability relationship to match the scale of the reservoir grid block.

Methodology used:

Quasi-point porosity permeability relationships applied to single well micro scale models. These are then coarsened in a way that preserves flow characteristics. To the scale shared by the macro reservoir model. The porosity permeability relationship from the upscaled model is then extracted and applied to the macro-scale model.

Conclusion reached:

Effective permeability becomes more strongly anisotropic as volume support increases from core plug scales which are larger than the heterogeneities which affect fluid flow from such laminations.

High end point estimates for kv/kh ratio are produced when core based poroperm relationships are used at macro scale reservoir models.

Comment: Methodology successfully applied to the Hamaca reservoir, Venezuela.

SPE 143613-MS (2011)

Modeling the Interfering Effects of Gas Condensate and Geological Heterogeneities on Transient Pressure Response

Authors: H. Hamdi, M. Jamiolahmady and P.W.M. Corbett, Heriot-Watt U.

Contribution to the understanding of the influence of geology in gas condensate well-test interpretations

Objective of the paper:

Conducting sensitivities using numerical well test approach to evaluate the combined effect of geology and condensate dropout on well test responses.

Methodology used:

Single well sector model to carry out numerical well test analysis.

Conclusion reached:

- Increasing geology effect (heterogeneity) increases the 'ramp' response seen in fluvial reservoirs.
- Increasing vertical permeability causes the ramp response to disappear from the native geological well-test response
- Shorter correlations lengths magnifies the ramp effect

Comment:

Heterogeneous commingled reservoirs were only considered where kv=0.

SPE 36882 (1996)

A method for using the naturally-occurring negative geoskin in the description of fluvial reservoirs

Authors: Corbett, Patrick W.M., Heriot-Watt University; Mesmari, Abdallah, Agip Oil Co.; Stewart, George, Edinburgh Petroleum Services Ltd.

Contribution to the understanding negative skin in highly heterogeneous reservoirs that are typical of braided fluvial systems

Objective of the paper:

Interpretation of skin in braided fluvial reservoirs.

Methodology used:

Sector model to carry out numerical well test analysis and results interpreted with well test package. Pseudo fracture channel phenomena was investigated.

Conclusion reached:

- Geoskin can be expected in braided fluvial systems where high permeability and small scale channels are present

SPE 93992-MS (2005)

The geochoke well test response in a catalogue of systematic geotype curves

Authors: P.W.M. Corbett, SPE, Y. Ellabad, J.I.K. Egert, and S. Zheng, SPE, Heriot-Watt University

Contribution to identifying the geochoke well test response

Objective of the paper:

Identifying the geochoke well test response in two field examples, more importantly for braided fluvial reservoirs.

Methodology used:

Black oil model was used to run stochastic realizations of varying correlation lengths. Pressures build up and drawdowns are simulated. Well test analysis is conducted on the build ups.

Conclusion reached:

- For shorter correlation lengths the hump response is more common
- As the correlations lengths increase, the hump response becomes rare and disappears.

Appendix C

Reservoir Analysis and Simulation

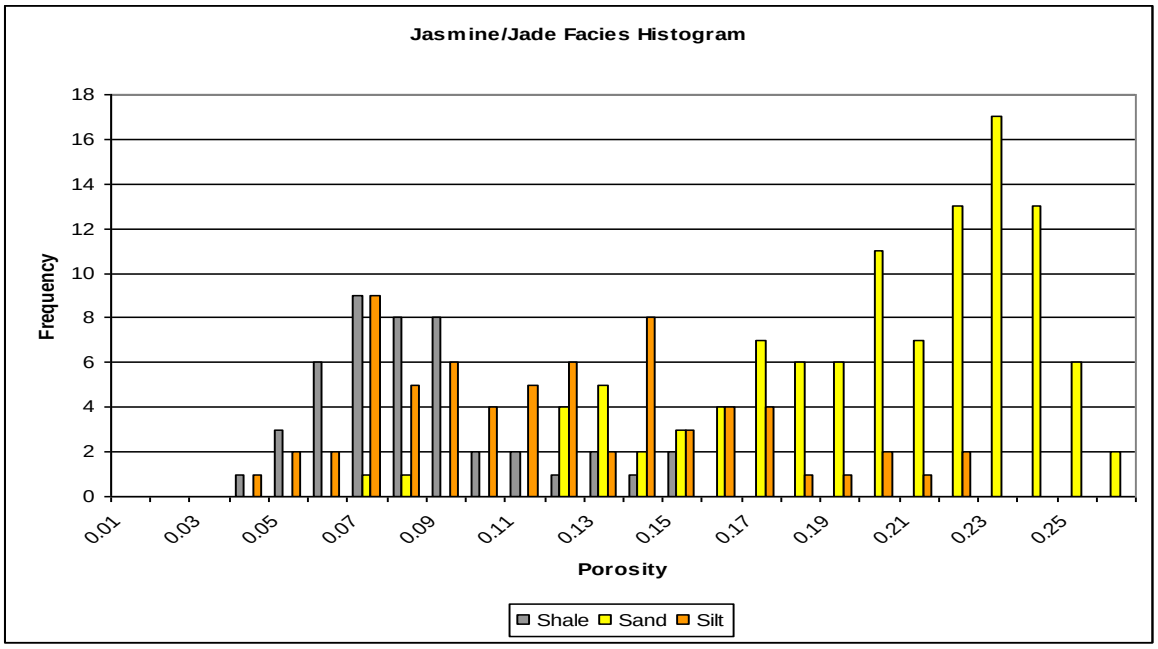

Figure C- 1: Distribution of porosity by individual facies types, statistical distribution was fitted to data and used to populate porosity in the model

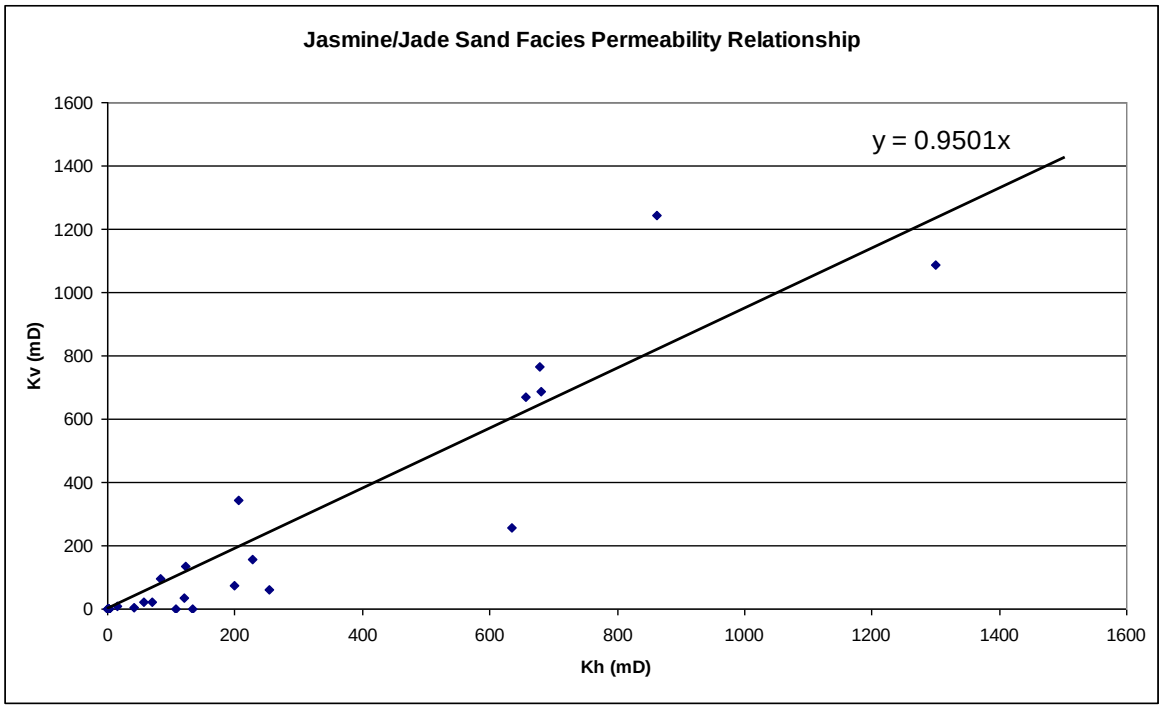

Figure C- 2: Kv-Kh relationship for sand facies, a strong correlation

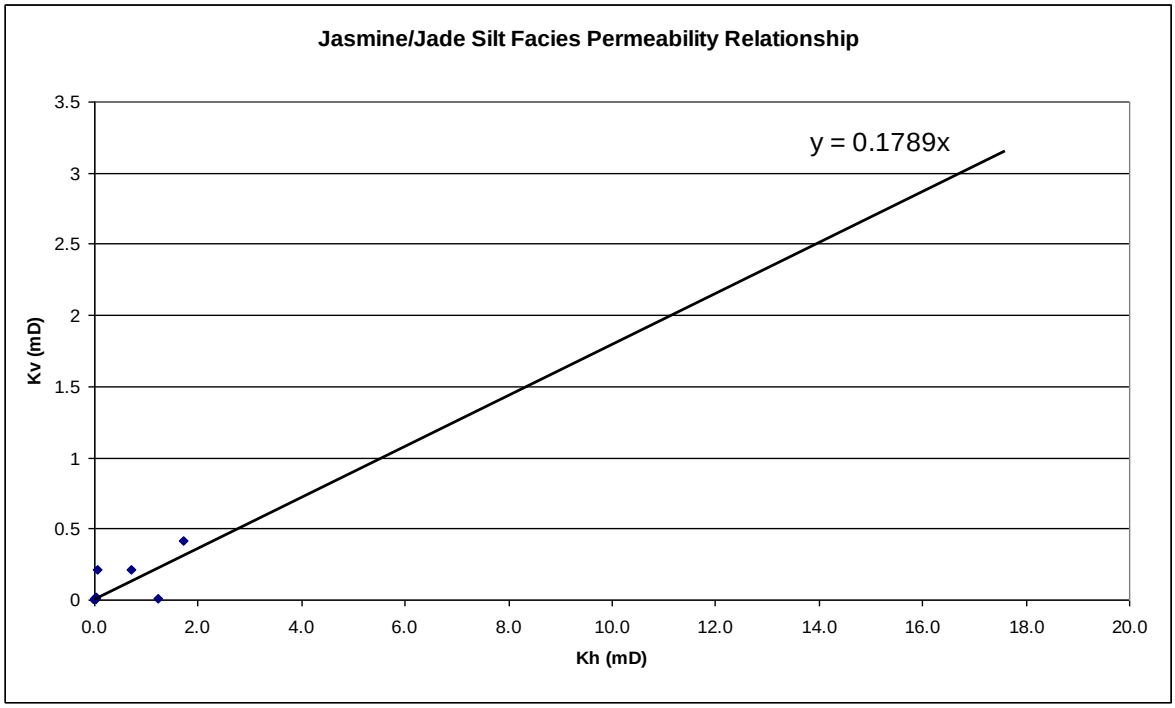

Figure C- 3: Kv-Kh relationship for silt facies, poor correlation is observed with very limited data points

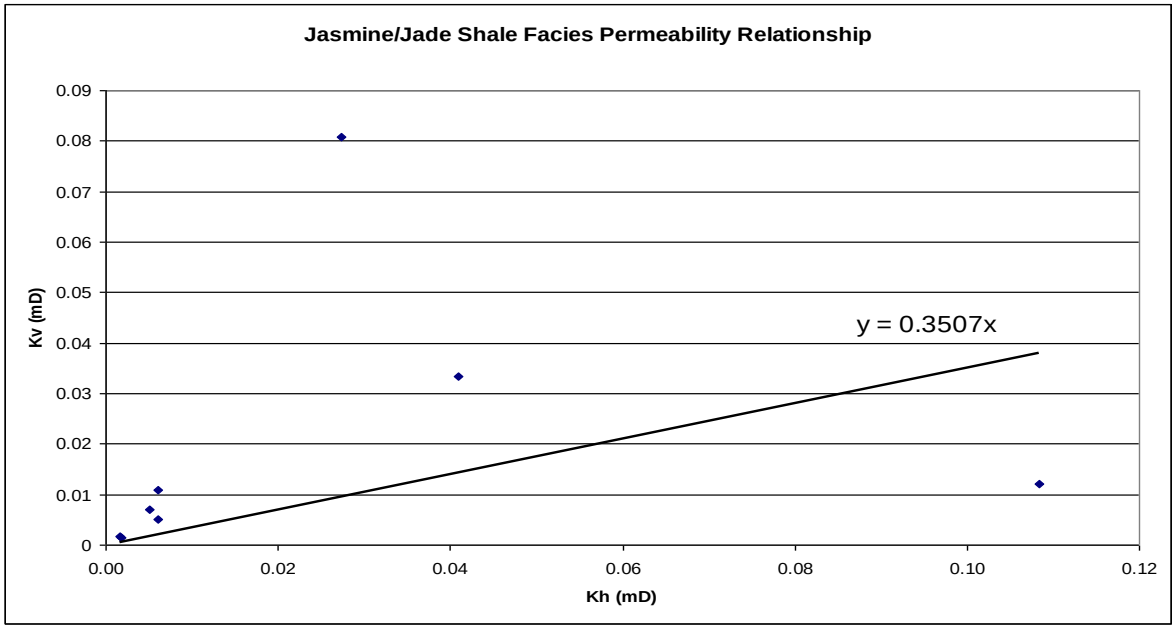

Figure C- 4: Kv-Kh relationship for shale facies, again poor relationship is observed with very limited data points

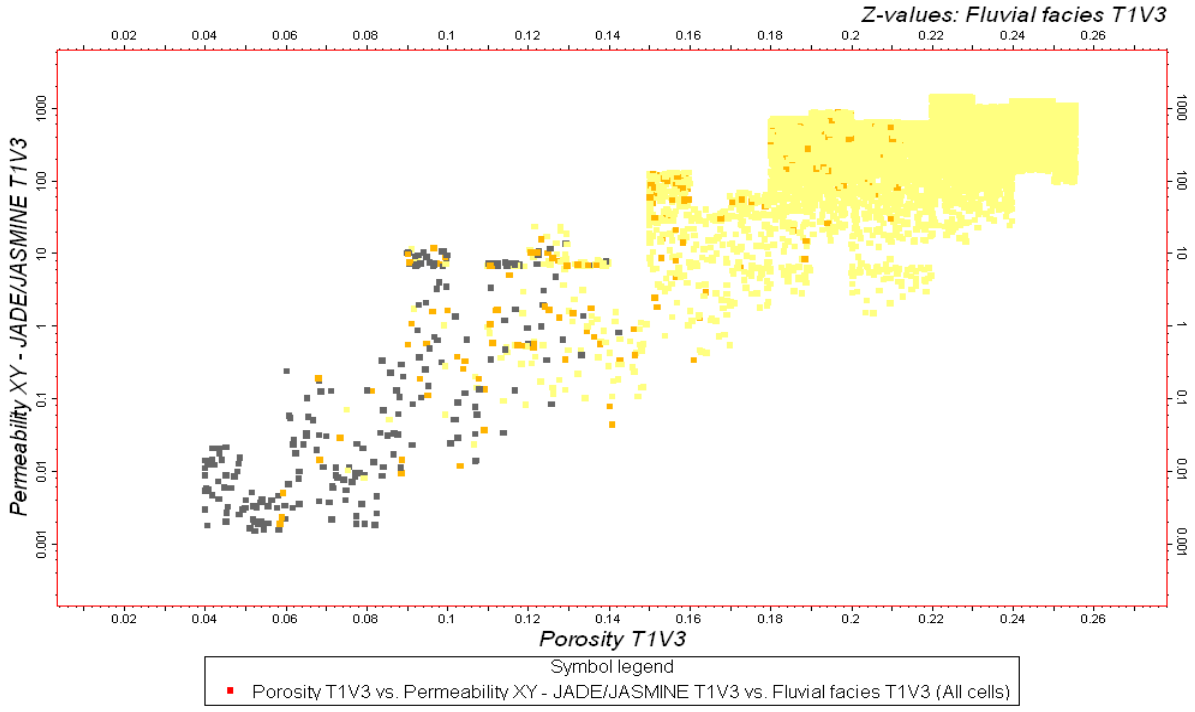

Figure C- 5: Cloud transform derived from Jade/Jasmine data set, over a 1000 points are plotted showing the high level of skew at the top end of the sand cloud. Shales are represented by the grey points, silts by orange and sand by yellow points.

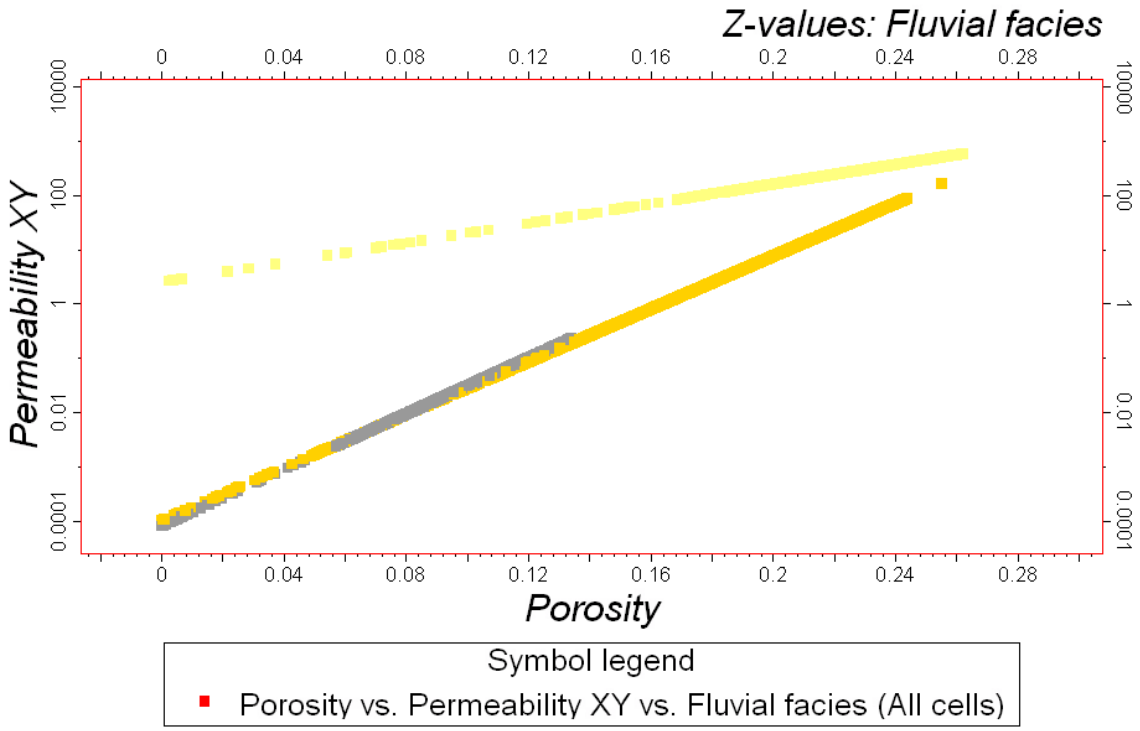

Figure C- 6: Jasmine/Jade linear poroperm relationship.

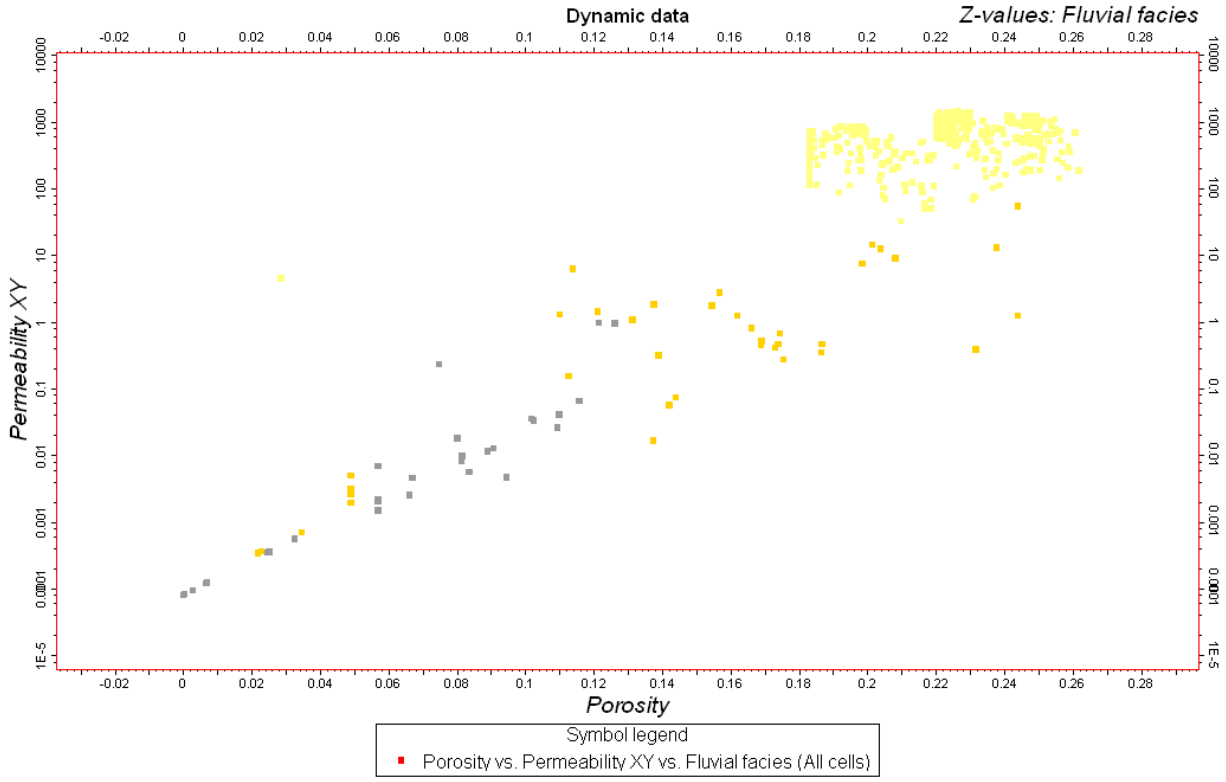

Figure C-7: Comparison of Jade core plug data against generated Jade poroperm cloud transform. Shales are represented by the grey points, silts by orange and sand by yellow points for the generated cloud transform.

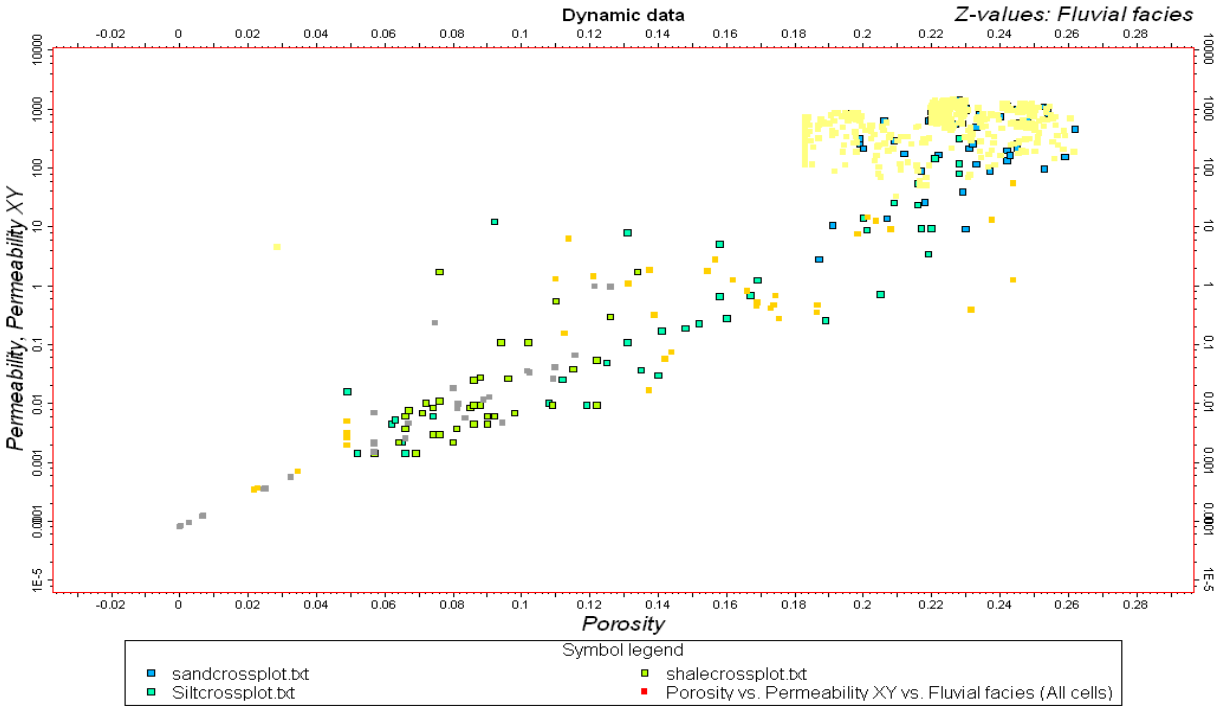

Figure C-8: Poroperm Cloud transform derived from core Jade data, under 500 points plotted. Shales are represented by the grey points, silts by orange and sand by yellow points.

Linear Poroperm Transform Plots

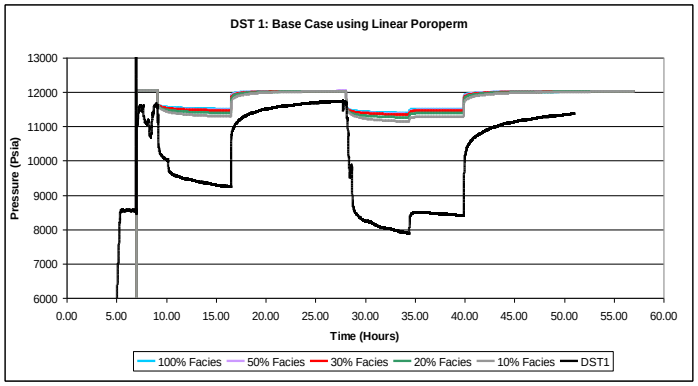

Figure C-9: PBU showing sensitivity of five different correlation lengths without using multipliers

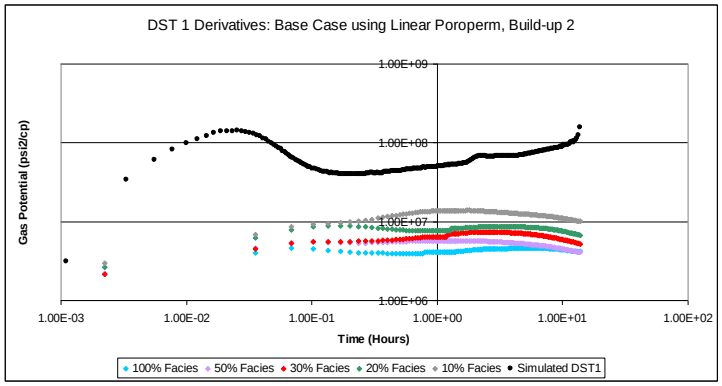

Figure C-10: Derivatives showing sensitivity of five different correlation lengths without using multipliers

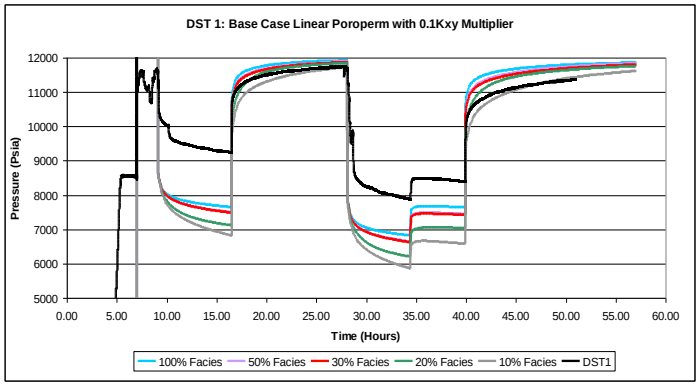

Figure C-11: PBU showing sensitivity of five different correlation lengths using 0.1 Kxy multiplier

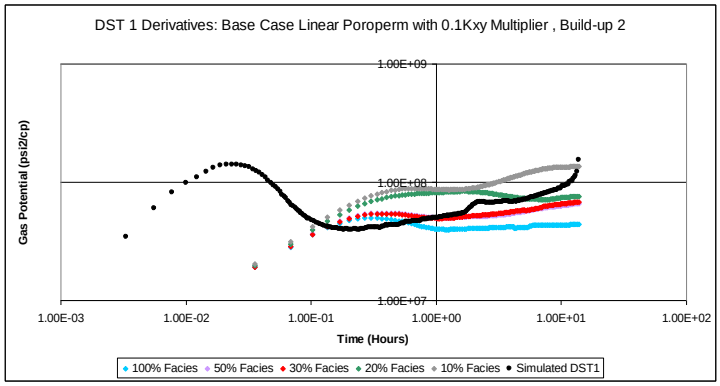

Figure C-12: Derivative showing sensitivity of five different correlation lengths using 0.1 Kxy multiplier

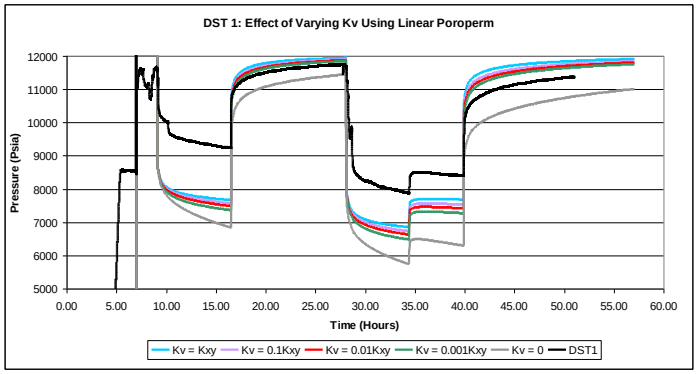

Figure C-13: PBU showing Kv sensitivity using 30% correlation lengths

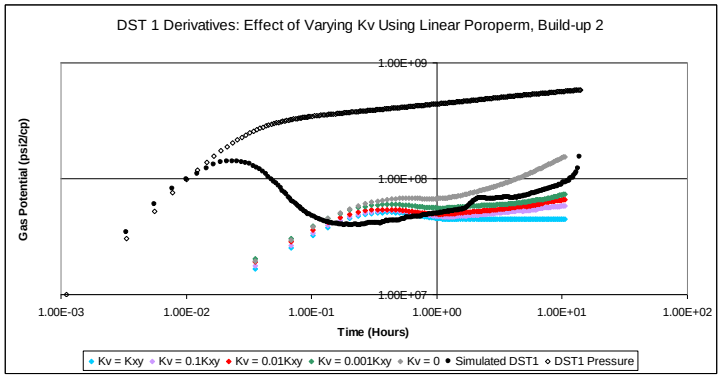

Figure C-14: Derivatives showing Kv sensitivity using 30% correlation lengths

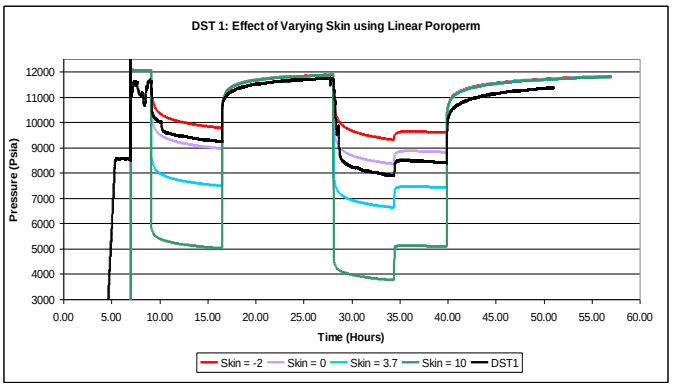

Figure C-15: PBU showing Skin sensitivity using 30% correlation lengths

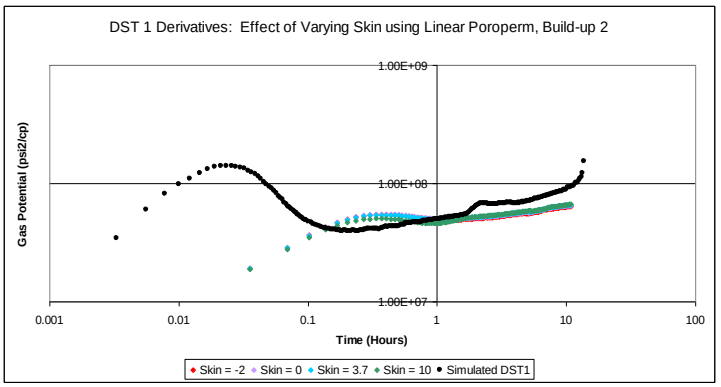

Figure C-16: Derivatives showing Skin sensitivity using 30% correlation lengths

Appendix D

Fine Grid Model Example Simulation Deck

```
RUNSPEC
  AQUDIMS
  2 2 1 36 2 4000 2* /
  TITLE
  FGM_T1V1
  WELLDIMS
   1* 1* 2 1 /
  START
    1 JAN 2011 /
  WATER
  GAS
  PETOPTS
  INITNNC EDITSUPP /
  MONITOR
  MULTOUT
  FIELD

  DIMENS
    160 160 20 /
  TABDIMS
    1 1 20 20 1* 20 20 5* 1 /
GRID
  INCLUDE
 ******** START OF INCLUDED FILE FGM_T1V1_GRID.INC
```

```
  AQUCON
   1 1 1 1 160 1 20 I- 1 0 NO /
   2 160 160 1 160 1 20 I+ 1 0 NO /
  /
  AQUNUM
   1 1 80 10 1.0E+10 20000 1* 200 1* 625 1 1 /
   2 160 80 10 1.0E+10 20000 1* 200 1* 300 1 1 /
  /
  INIT
  GRIDFILE
    0 0 /
  GRIDUNIT
    FEET /

  MAPUNITS
    FEET /
  MAPAXES
    0.00 -840.00 0.00 160.00 1000.00 160.00 /
  PINCH
    /
 ******** END OF INCLUDED FILE
  NOECHO
  ECHO
  EDIT
PROPS
  INCLUDE
 ******** START OF INCLUDED FILE FGM_T1V1_PROPS.INC
  ROCKOPTS
```

```
  1* 1* ROCKNUM /
ROCK
           400  1.4234E-005 /

PVTW
        3118.3       1.0132  2.7438E-006      0.39851            0 /
RVCONSTT
             0       1160.3 /
PVDG
        1160.3       2.4888      0.01446
        1356.1       2.1052     0.014928
        1551.9       1.8216     0.015439
        1747.7       1.6047     0.015991
        1943.5       1.4344     0.016581
        2139.3       1.2981     0.017206
        2335.1       1.1872      0.01786
        2530.9       1.0959      0.01854
        2726.7       1.0197      0.01924
        2922.5      0.95565     0.019954
        3118.3      0.90125     0.020678
        3314.1      0.85469     0.021408
        3509.9      0.81452     0.022139
        3705.7      0.77962     0.022869
        3901.5      0.74908     0.023594
        4097.3      0.72218     0.024313
        4293.1      0.69833     0.025024
        4488.9      0.67707     0.025727
        4684.7      0.65801     0.026419
```

```
        4880.5      0.64083     0.027101
  /
DENSITY
  1*       63.698     0.050674 /
FILLEPS
SGFN
             0            0            0
          0.05            0            0
        0.1412            0            0
        0.2325       0.0002            0
        0.3237       0.0021            0
         0.415        0.012            0
        0.5062       0.0456            0
        0.5975       0.1362            0
        0.6887       0.3434            0
          0.78       0.7653            0
           0.8          0.9            0
  /
SWFN
           0.2            0            0
          0.22            0            0
        0.3113       0.0002            0
        0.4025       0.0031            0
        0.4938       0.0158            0
         0.585         0.05            0
        0.6763       0.1221            0
        0.7675       0.2531            0
        0.8588       0.4689            0
```

```
            0.95          0.8            0
               1            1            0
    /
 ******** END OF INCLUDED FILE
  REGIONS
  NOECHO
  ECHO
  SOLUTION
  INCLUDE
 ******** START OF INCLUDED FILE FGM_T1V1_SOL.INC
  RPTRST
    BASIC=3 FLOWS FREQ=200 VISC KRW SWAT /
  RPTSOL
    RESTART=2 FIP /
 ******** END OF INCLUDED FILE
  SUMMARY
  INCLUDE
 ******** START OF INCLUDED FILE FGM_T1V1_SUM.INC
SCHEDULE
 INCLUDE
 ******** START OF INCLUDED FILE FGM_T1V1_SCH.INC
```

Full Field Model Simulation Deck – Example Grid: 30%, DST1 Lower Joanne

```
RUNSPEC
  TITLE
  DST2_BC_S10_G3_E300
  WELLDIMS
  1 13 2 1 1* 1* 1* 1* 1* 1* 1* 1* 10 /
  START
    1 JAN 1995 /
  WATER
  PETOPTS
  MONITOR
  MULTSAVE
    -1 /
  MULTOUT
  FIELD
  DIMENS
  50 50 326 /
  TABDIMS
    1 2 43 5* 2 1* 1* 1* 1 /
  COMPS
    7 /
  EQLDIMS
    2 /
 GRID
  INCLUDE
******** START OF INCLUDED FILE DST2_BC_S10_G3_E300_GRID.INC
  INIT
  GRIDFILE
```

```
    0 0 /
  GRIDUNIT
    FEET /
  MAPUNITS
    FEET /
  MAPAXES
    0.00 0.00 0.00 3280.84 3280.84 3280.84 /
  PINCH
    /
 ******** END OF INCLUDED FILE DST2_BC_S10_G3_E300_GRID.INC
  NOECHO
 ******** START OF INCLUDED FILE DST2_BC_S10_G3_E300_GRID.GRDECL
 ******** END OF INCLUDED FILE DST2_BC_S10_G3_E300_GRID.GRDECL
 ******** START OF INCLUDED FILE DST2_BC_S10_G3_E300_PROP_PERMX.GRDECL
 ******** END OF INCLUDED FILE DST2_BC_S10_G3_E300_PROP_PERMX.GRDECL
 ******** START OF INCLUDED FILE DST2_BC_S10_G3_E300_PROP_PERMY.GRDECL
 ******** END OF INCLUDED FILE DST2_BC_S10_G3_E300_PROP_PERMY.GRDECL
 ******** START OF INCLUDED FILE DST2_BC_S10_G3_E300_PROP_PERMZ.GRDECL
 ******** END OF INCLUDED FILE DST2_BC_S10_G3_E300_PROP_PERMZ.GRDECL
 ******** START OF INCLUDED FILE DST2_BC_S10_G3_E300_PROP_PORO.GRDECL
 ******** END OF INCLUDED FILE DST2_BC_S10_G3_E300_PROP_PORO.GRDECL
  EDIT
PROPS
  INCLUDE
 ******** START OF INCLUDED FILE DST2_BC_S10_G3_E300_PROPS.INC
  EOS
    PR /
    PR /
```

```
 PRCORR
 CNAMES
   C1N2
CO2C2
C3C4
C5C6
C7P
C14P
C28P
/
 TCRIT
   342.24 548.99 703.22 872.08 1002.26 1320.05 1788.84 /
   341.60 549.05 706.03 872.92 1068.94 1356.49 1745.99 /
 PCRIT
   665.9327 830.1473 584.6957 462.7556 354.3218 229.6221 176.3915 /
   664.9579 821.1849 582.6939 462.4064 342.6301 228.6085 177.7416 /
 VCRIT
   1.60800 2.07900 3.62700 5.36400 9.32100 18.03800 40.88201 /
   1.70200 2.10100 3.65200 5.36900 9.64500 18.18100 38.32501 /
 ZCRIT
   0.29161 0.29297 0.28101 0.26523 0.30705 0.29238 0.37563 /
   0.30881 0.29277 0.28086 0.26500 0.28807 0.28551 0.36354 /
 MW
   16.09 33.66 49.15 81.78 123.02 250.87 527.68 /
   16.13 33.37 49.54 81.23 128.36 252.77 504.06 /
 ACF
   0.00823 0.14079 0.16676 0.2652 0.43866 0.79975 1.14971 /
   0.00841 0.13764 0.1679 0.26613 0.45401 0.77101 0.99551 /
```

```
OMEGAA
  7*0.45723553 /
  7*0.45723553 /
OMEGAB
  7*0.077796074 /
  7*0.077796074 /
SSHIFT
  -0.193967 -0.113202 -0.10358 -0.02981 0.042482 0.046618 -0.113321 /
  -0.086515 -0.116392 -0.102928 -0.028715 0.084036 0.06812 -0.104825 /
BIC
  6*0.0 0.039263996 0.01 0.01 0.0 0.0512734 0.01 0.01 0.0 0.0
  0.061353654 0.01 0.01 0.0 0.0 0.0 /
  6*0.0 0.040069375 0.01 0.01 0.0 0.051383361 0.01 0.01 0.0 0.0
  0.060781695 0.01 0.01 0.0 0.0 0.0 /
PARACHOR
  77.037 98.489 167.232 248.547 357.786 672.183 1377.878 /
  76.835 99.255 168.362 249 368.949 676.655 1304.363 /
TEMPVD
  14900.00 370.00
  /
  15500.00 381.00
  /
ZMFVD
  14900.00
  0.822754 0.093104 0.036332 0.011361 0.024278 0.009458 0.002713
  /
  15500.00
  0.726188 0.108574 0.058206 0.021129 0.053286 0.026354 0.006263
```

```
  /
PVTW
          2000            1       3E-006         0.35       4E-006 /
          2000            1       3E-006         0.35       4E-006 /
DENSITY
  1*         62.4 /
  1*         62.4 /
ROCKOPTS
  1* 1* ROCKNUM /
ROCK
          2000       4E-006 /
FILLEPS
SWOF
          0.16            0            1       11.271
         0.165            0      0.98118       10.372
          0.17            0      0.96236        9.569
         0.175            0      0.94355        8.849
          0.18            0      0.92473        8.201
         0.185            0      0.90591        7.616
          0.19            0      0.88709        7.087
         0.195            0      0.86828        6.607
           0.2            0      0.84946         6.17
         0.205            0      0.83064        5.772
          0.21            0      0.81182        5.409
         0.215            0        0.793        5.076
          0.22            0      0.77419         4.77
         0.225            0      0.75537        4.489
          0.23            0      0.73655        4.231
```

```
          0.235            0      0.71773        3.992
           0.24            0      0.69891        3.772
          0.245            0       0.6801        3.567
           0.25            0      0.66128        3.378
            0.3            0       0.4731        2.065
           0.35   0.00079942      0.35057        1.362
         0.3688       0.0011       0.3045       1.2071
            0.4    0.0034616      0.24937         0.95
         0.4375       0.0063       0.1831      0.75575
           0.45    0.0082804      0.16806        0.691
            0.5     0.016202      0.10788         0.52
         0.5063       0.0172       0.1003      0.50513
           0.55     0.028777     0.067032        0.402
          0.575       0.0354        0.048         0.36
            0.6     0.045007     0.037301        0.318
         0.6437       0.0618       0.0186      0.26381
           0.65      0.06506     0.017345        0.256
            0.7     0.090932    0.0073891         0.21
         0.7125       0.0974       0.0049        0.201
           0.75       0.1224    0.0024983        0.174
         0.7812       0.1432       0.0005      0.15653
            0.8      0.15872   0.00036337        0.146
           0.85          0.2            0        0.124
              1            1            0         0.08
  /


SGOF
              0            0            1            0
```

```
          0.11            0       0.4703            0
        0.1763       0.0078       0.2757            0
        0.2425       0.0313       0.1488            0
        0.3088       0.0703       0.0718            0
         0.375        0.125       0.0294            0
          0.42      0.17271     0.015757            0
        0.4413       0.1953       0.0093            0
        0.5075       0.2813       0.0018            0
        0.5738       0.3828       0.0001            0
          0.64          0.5            0            0
          0.84            1            0            0
   /
 ******** END OF INCLUDED FILE DST2_BC_S10_G3_E300_PROPS.INC
REGIONS
  NOECHO
 ******** START OF INCLUDED FILE DST2_BC_S10_G3_E300_PROP_SATNUM.GRDECL
 ******** END OF INCLUDED FILE DST2_BC_S10_G3_E300_PROP_SATNUM.GRDECL
 ******** START OF INCLUDED FILE DST2_BC_S10_G3_E300_PROP_ROCKNUM.GRDECL
 ******** END OF INCLUDED FILE DST2_BC_S10_G3_E300_PROP_ROCKNUM.GRDECL
 ******** START OF INCLUDED FILE DST2_BC_S10_G3_E300_PROP_EOSNUM.GRDECL
 ******** END OF INCLUDED FILE DST2_BC_S10_G3_E300_PROP_EOSNUM.GRDECL
 ******** START OF INCLUDED FILE DST2_BC_S10_G3_E300_PROP_PVTNUM.GRDECL
 ******** END OF INCLUDED FILE DST2_BC_S10_G3_E300_PROP_PVTNUM.GRDECL
 ******** START OF INCLUDED FILE DST2_BC_S10_G3_E300_PROP_EQLNUM.GRDECL
 ******** END OF INCLUDED FILE DST2_BC_S10_G3_E300_PROP_EQLNUM.GRDECL
SOLUTION
  INCLUDE
 ******** START OF INCLUDED FILE DST2_BC_S10_G3_E300_SOL.INC
```

```
  FIELDSEP
    1 195 560 /
    2 60.0000008 14.6959487755135 /
    /
  EQUIL
           14900        12250        17850            0        17850
               0 0 0 0 1 /
           15500        12350        17850            0        17850
               0 0 0 0 1 /
  RPTRST
    BASIC=3 FREQ=1600 SGAS SOIL SWAT /
  RPTSOL
    FIP /
 ******** END OF INCLUDED FILE DST2_BC_S10_G3_E300_SOL.INC
SUMMARY
  INCLUDE
 ******** START OF INCLUDED FILE DST2_BC_S10_G3_E300_SUM.INC
 ******** END OF INCLUDED FILE DST2_BC_S10_G3_E300_SUM.INC
SCHEDULE
  INCLUDE
 ******** START OF INCLUDED FILE DST2_BC_S10_G3_E300_SCH.INC
  RPTSCHED
    FIP /
  RPTRST
    BASIC=3 FREQ=1600 SGAS SOIL SWAT /
  DATES
    1 JAN 1995 07:000 /
    /
```

```
 SKIP
 --Hint: Select wells on the input tree, drop in with the blue arrow, then ad
1& dd rules with the rule pop-up
 ENDSKIP
 WELSPECS
 --'30/2/4C' is the simulation well name used to describe flow from '30/2/4C'
 --
   '30/2/4C' 'GROUP 1' 25 26 13996.00 OIL /
   /
 COMPDAT
   '30/2/4C' 25 26 14 14 OPEN 1* 0.0023 0.62500 4.37 10.00 1* Z 12.99 /
   '30/2/4C' 25 26 15 15 OPEN 1* 0.6886 0.62500 1334.71 10.00 1* Z 12.99
   /
   '30/2/4C' 25 26 16 16 OPEN 1* 1.5025 0.62500 2912.43 10.00 1* Z 12.99
   /
   '30/2/4C' 25 26 17 17 OPEN 1* 1.0706 0.62500 2075.34 10.00 1* Z 12.99
   /
   '30/2/4C' 25 26 18 18 OPEN 1* 0.4163 0.62500 807.00 10.00 1* Z 12.99 /
   '30/2/4C' 25 26 19 19 OPEN 1* 0.8933 0.62500 1731.49 10.00 1* Z 12.99
   /
   '30/2/4C' 25 26 20 20 OPEN 1* 1.0906 0.62500 2113.99 10.00 1* Z 12.99
   /
   '30/2/4C' 25 26 21 21 OPEN 1* 0.3280 0.62500 635.72 10.00 1* Z 12.99 /
   '30/2/4C' 25 26 22 22 OPEN 1* 0.4248 0.62500 823.40 10.00 1* Z 12.99 /
   '30/2/4C' 25 26 23 23 OPEN 1* 0.3917 0.62500 759.30 10.00 1* Z 12.99 /
   '30/2/4C' 25 26 24 24 OPEN 1* 2.0326 0.62500 3940.03 10.00 1* Z 12.99
   /
   '30/2/4C' 25 26 25 25 OPEN 1* 0.0006 0.62500 1.20 10.00 1* Z 12.99 /
```

```
  '30/2/4C' 25 26 326 326 OPEN 1* 0.0082 0.62500 4.33 0.00 1* Z 12.99 /
  /
WRFTPLT
  '30/2/4C' REPT NO NO /
  /
GRUPTREE
  'GROUP 1' FIELD /
  /
WCONHIST
  '30/2/4C' STOP GRAT 0.00 1* 0.00 /
  /
```

Appendix E

Sample Macro used to build poroperm cloud transform for a single realisation in the fine grid model

Variogram_1\TEST_1\Permeability_XY_JADE_JASMINE_T1V1=if(Variogram_1\TEST_1\Porosity_T1V1>0.04 and Variogram_1\TEST_1\Porosity_T1V1<=0.06, TruncLogNormal(0.00329042481, 0.00362667493, 0.00141904895 , 0.0412501382), Variogram_1\TEST_1\Permeability_XY_JADE_JASMINE_T1V1)

Variogram_1\TEST_1\Permeability_XY_JADE_JASMINE_T1V1=if(Variogram_1\TEST_1\Porosity_T1V1>0.06 and Variogram_1\TEST_1\Porosity_T1V1<=0.08, TruncLogNormal(0.0179341366, 0.0535809186, 0.00142319531 , 1.73361548), Variogram_1\TEST_1\Permeability_XY_JADE_JASMINE_T1V1)

Variogram_1\TEST_1\Permeability_XY_JADE_JASMINE_T1V1=if(Variogram_1\TEST_1\Porosity_T1V1>0.08 and Variogram_1\TEST_1\Porosity_T1V1<=0.1, TruncLogNormal(0.0412347889, 0.125505327, 0.00176740727 , 12.1044448), Variogram_1\TEST_1\Permeability_XY_JADE_JASMINE_T1V1)

Variogram_1\TEST_1\Permeability_XY_JADE_JASMINE_T1V1=if(Variogram_1\TEST_1\Porosity_T1V1>0.1 and Variogram_1\TEST_1\Porosity_T1V1<=0.12, TruncLogNormal(0.53247909, 0.949274848, 0.00929080307 , 7.45995663), Variogram_1\TEST_1\Permeability_XY_JADE_JASMINE_T1V1)

Variogram_1\TEST_1\Permeability_XY_JADE_JASMINE_T1V1=if(Variogram_1\TEST_1\Porosity_T1V1>0.12 and Variogram_1\TEST_1\Porosity_T1V1<=0.14, TruncLogNormal(0.413153719, 0.660618425, 0.00849599142 , 24.2046857), Variogram_1\TEST_1\Permeability_XY_JADE_JASMINE_T1V1)

Variogram_1\TEST_1\Permeability_XY_JADE_JASMINE_T1V1=if(Variogram_1\TEST_1\Porosity_T1V1>0.14 and Variogram_1\TEST_1\Porosity_T1V1<=0.16, TruncLogNormal(0.922379883, 1.37279614, 0.0297941402 , 129.131307), Variogram_1\TEST_1\Permeability_XY_JADE_JASMINE_T1V1)

Variogram_1\TEST_1\Permeability_XY_JADE_JASMINE_T1V1=if(Variogram_1\TEST_1\Porosity_T1V1>0.16 and Variogram_1\TEST_1\Porosity_T1V1<=0.18, TruncLogNormal(4.05017731, 6.31819643, 0.217099369 , 67.353551), Variogram_1\TEST_1\Permeability_XY_JADE_JASMINE_T1V1)

Variogram_1\TEST_1\Permeability_XY_JADE_JASMINE_T1V1=if(Variogram_1\TEST_1\Porosity_T1V1>0.18 and Variogram_1\TEST_1\Porosity_T1V1<=0.2, TruncLogNormal(267.437605, 231.633615, 0.25406667 , 863.99386), Variogram_1\TEST_1\Permeability_XY_JADE_JASMINE_T1V1)

Variogram_1\TEST_1\Permeability_XY_JADE_JASMINE_T1V1=if(Variogram_1\TEST_1\Porosity_T1V1>0.2 and Variogram_1\TEST_1\Porosity_T1V1<=0.22, TruncLogNormal(178.657358, 211.016148, 0.709735757 , 637.567502), Variogram_1\TEST_1\Permeability_XY_JADE_JASMINE_T1V1)

Variogram_1\TEST_1\Permeability_XY_JADE_JASMINE_T1V1=if(Variogram_1\TEST_1\Porosity_T1V1>0.22 and Variogram_1\TEST_1\Porosity_T1V1<=0.24, TruncLogNormal(464.34182, 395.228118, 9.13942523 , 1432.54758), Variogram_1\TEST_1\Permeability_XY_JADE_JASMINE_T1V1)

Variogram_1\TEST_1\Permeability_XY_JADE_JASMINE_T1V1=if(Variogram_1\TEST_1\Porosity_T1V1>0.24 and Variogram_1\TEST_1\Porosity_T1V1<=0.262, TruncLogNormal(574.52022, 385.969407, 95.9074815 , 1238.52144), Variogram_1\TEST_1\Permeability_XY_JADE_JASMINE_T1V1)

Variogram_1\TEST_1\Permeability_Z_JADE_JASMINE_T1V1=if(Variogram_1\TEST_1\Fluvial_facies_T1V1=0,0.3507*Variogram_1\TEST_1\Permeability_XY_JADE_JASMINE_T1V1,Variogram_1\TEST_1\Permeability_Z_JADE_JASMINE_T1V1)

Variogram_1\TEST_1\Permeability_Z_JADE_JASMINE_T1V1=if(Variogram_1\TEST_1\Fluvial_facies_T1V1=1,0.9501*Variogram_1\TEST_1\Permeability_XY_JADE_JASMINE_T1V1,Variogram_1\TEST_1\Permeability_Z_JADE_JASMINE_T1V1)

Variogram_1\TEST_1\Permeability_Z_JADE_JASMINE_T1V1=if(Variogram_1\TEST_1\Fluvial_facies_T1V1=2,0.1789*Variogram_1\TEST_1\Permeability_XY_JADE_JASMINE_T1V1,Variogram_1\TEST_1\Permeability_Z_JADE_JASMINE_T1V1)